Usage of SERC SahasraT Supercomputer for Scientific Applications in IISc in 2018

Supercomputer Education and Research Centre

Indian Institute of Science

Bangalore – 560012

March 2019

Table of Contents

1. SERC Cray SahasraT System

SERC is home to one of the fastest supercomputers in India, the Cray XC40, known as SahasraT in IISc. It was commissioned in 2015. SahasraT is also the fastest academic supercomputer in India. It is a system that combines the capabilities of Intel's latest Xeon Haswell processors for the CPU cluster and Nvidia's K40 series of GPU cards and Intel's energy efficient Xeon Phi Knights Landing MIC processors as a cluster connected using Cray's own Aries high-speed interconnect on a dragonfly topology with DDN's high performance storage units.

It is a 1.4 PFlop system with 33000 Intel Haswell cores with total memory of 176 TB RAM, and 2 PB of storage. It also has 44 accelerator nodes each with one NVIDIA K40 GPU card, and 24 nodes each with one Intel Xeon KNL processors.

System also hosts architecture specific parallel libraries like OpenMP, MPI, CUDA and Intel Cluster software. Extensive range of parallel Scientific and Mathematical libraries like BLAS, LAPACK, Scalapack, fftw, hdf5, netcdf, PETSc, Trilinos etc. are also available on the system.

The CRAY XC40 facility uses PBS (Portable Batch System) to schedule jobs. The scheduler for batch jobs in SahsaraT uses the FCFS (First-Come, First-Served), based on queue priority and backfilling techniques to achieve the highest system utilization possible with a reasonable turn-around time.

There are eight regular queues configured on the Cray XC40 with limitations on job size in terms of cores requested, wall time and number of jobs on queue and in the running state. Large and medium jobs are prioritized, over small jobs.

2. Usage in 2018

SahasraT serves 37 Departments, 90 Research Labs and over 331 users. Following are some salient statistics of the usage of SahasraT in 2018.

- A total of 96334 jobs were processed in 2018, at an average of 8027 jobs per month. 84.07% of the jobs were CPU jobs and 15.5% of the jobs were GPU jobs, the remaining were jobs in in special queues like temporary queue or advance reservation queues.
- The total system utilization was about 248 Million core hours i.e., an average system utilization of about 20 million core hours per month.
- The overall availability and utilization for 2018 and usage by the different departments in 2018 is given in the following charts.

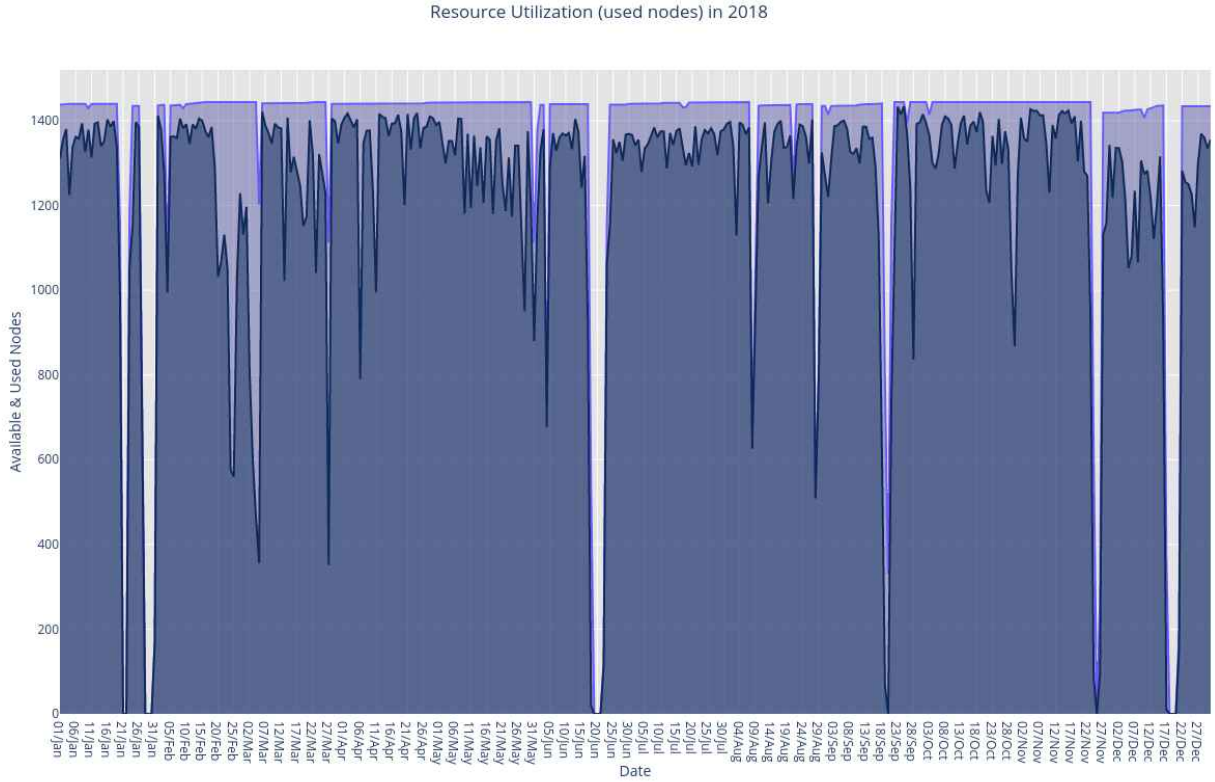
Resource Utilization (used nodes) in 2018
Available & Used Nodes
Date

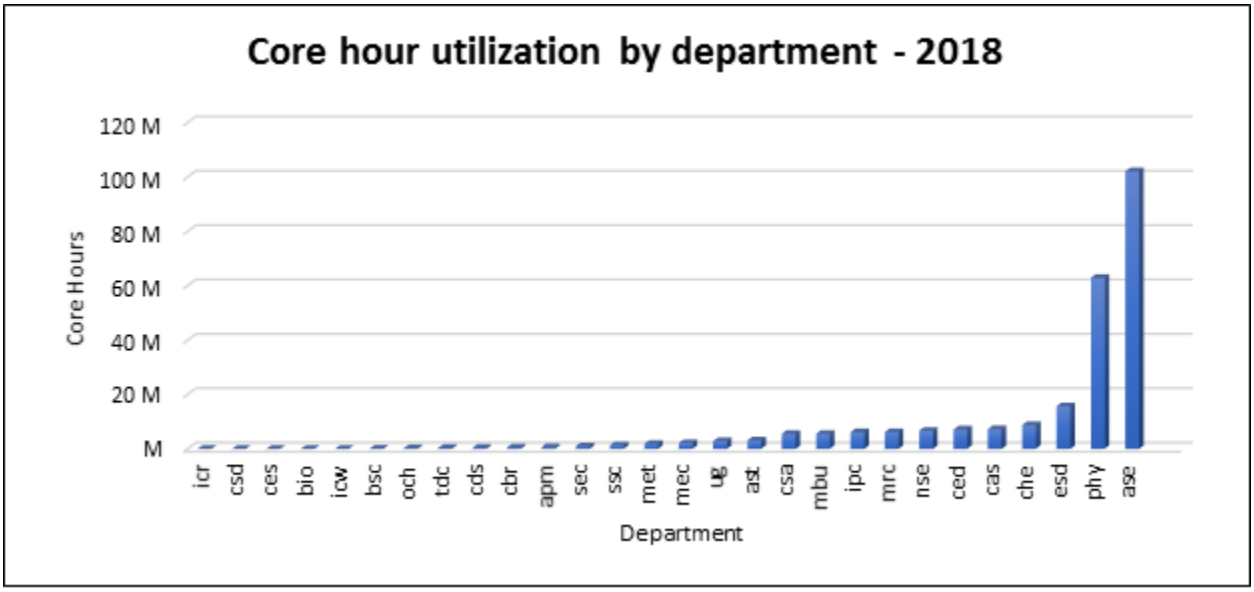
Core hour utilization by department - 2018
Core Hours
120 M
100 M
80 M
60 M
40 M
20 M
M
icr
csd
ces
bio
iow
bsc
och
tdc
cds
cbr
apm
sec
ssc
met
mec
ug
ast
csa
mbu
ipc
mrc
nse
ced
cas
che
esd
phy
ase
Department

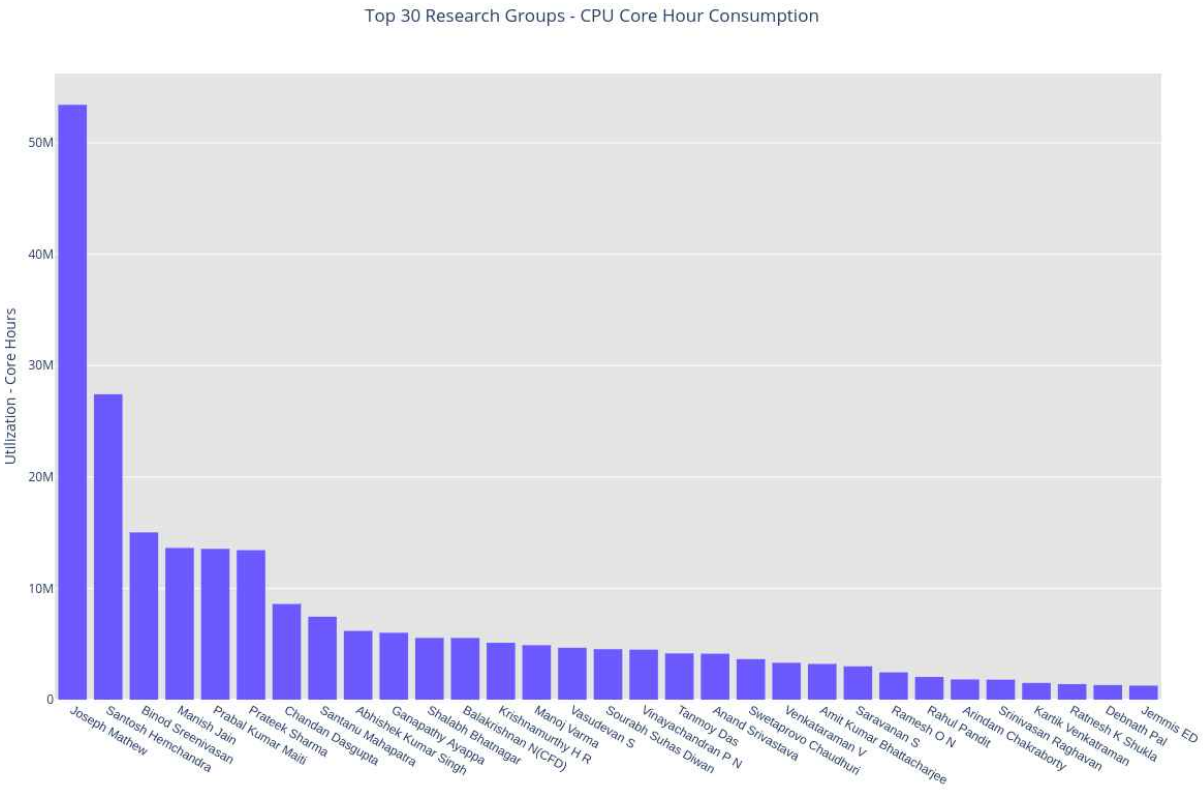

SahasraT queueing policies were refined in March 2018 to reduce queue wait times for large jobs, enabling more large job submissions on SahasraT from March 2018. The following chart provides resource utilization in terms of core hours per regular CPU Queue.

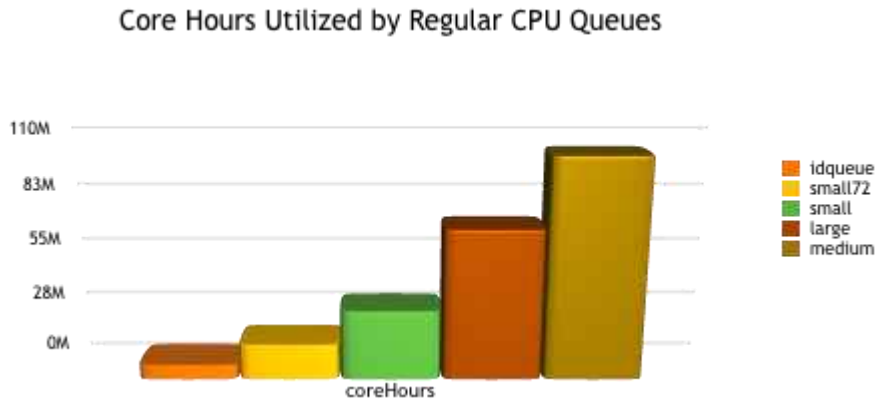

667 large jobs were processed in 2018 as opposed to only 26 large jobs in 2017.

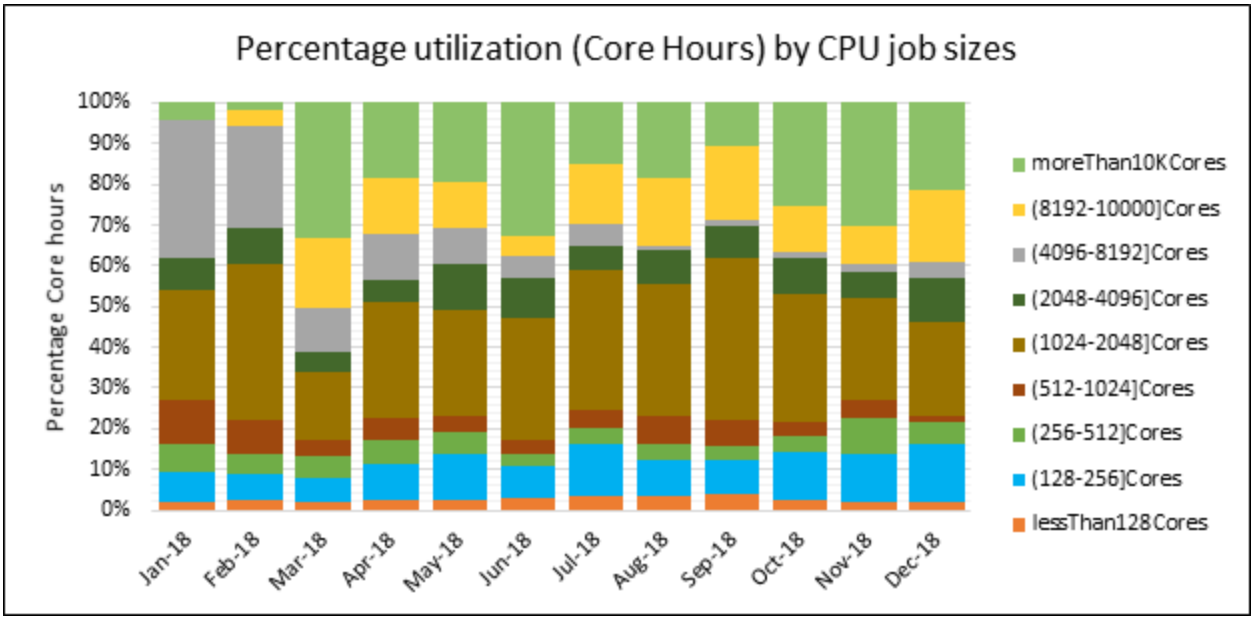

29.5 percent of the CPU hours were consumed by jobs using 1024 to 2048 cores, 19 percent of CPU hours were consumed by capability jobs using more than 10000 Cores and 11 percent of CPU hours were consumed by capability jobs using more than 8192 Cores.

3. IISc's Scientific Applications on SahasraT

In 2018, a large number of scientific applications were executed by the Institute community on SahasraT. These belonged to different departments including Aerospace, Physics, Centre for Atmospheric and Oceanic Sciences (CAOS), Centre for Brain Research (CBR), Department of Computational and Data Sciences (CDS), Chemical Engineering (CE), Centre for Earth Sciences (CEaS), Department of Computer Science and Automation (CSA), Department of Electronics Structure and Engineering (DESE), Inorganic and Physical Chemistry (IPC), Materials Engineering, Materials Research Centre (MRC), Molecular Biophysics Unit (MBU) and Mechanical Engineering. The applications spanned different domains including

- aerodynamics, turbulence computations,
- climate modelling,
- whole genome sequencing,
- study of proteins in breast cancer,
- large-scale finite element methods,
- large-scale graph problems,
- study of granular materials,
- Bayesian optimization methods,
- 2-D materials for lithium ion battery,
- interactions in halogen bond, carbon nanothreads,
- microstructure,
- study of biological membranes, analysis of conformational space of proteins,
- computational modelling of materials using machine learning,
- thermal transport in glass-forming liquids,

- study of band insulator,
- study of bilayer transition metal dichalcogenides (TMDs),
- study of biomolecules, glycoproteins, gene silencing mechanisms, dendrimer, DNA nanotubes,
- study of superfluid turbulence,
- etc.

The following sections gives details of the usage of SahasraT for various computational science problems.

3.1 Department of Aerospace Engineering (AE)

3.1.1 Prof. N Balakrishnan's Lab

Team: Computational Aerodynamics Lab

3.1.1.1 Research

(1) Unsteady aerodynamics: Dynamic derivaties, Scramjet intake flows, Time-step adaptive calculations, Active flow control (2) Optimization (3) Meshless solvers: Cartesian mesh calculations (4) High lift Aerodynamics (5) Propeller Aerodynamics.

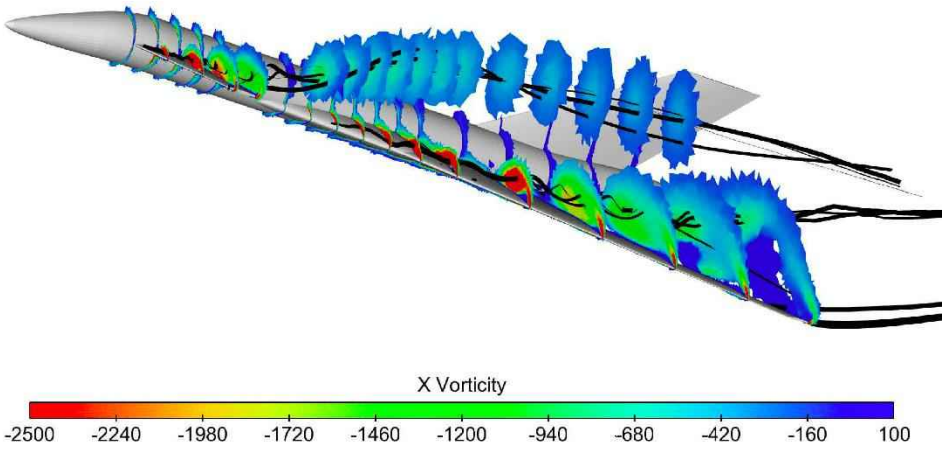

Transcruiser in Pitch Oscillation

3.1.1.2 Parallelization

MPI parallel HiFUN solver is used

3.1.1.3 SERC Resources and Experiments

In the year 2018, the problems considered were of two types; one involving less than million grid volumes (~ 500 K volumes), typically distributed on about 1000 cores, requiring about a month (run time) for completing the run and the other involving over 100 million volumes requiring about few days of computational effort on over 10000 cores. A good scalability of the solver is a prerequisite for both these types of usage. For example, the first type requires as less as 500 volumes per core, for accomplishing the run in a reasonable time frame. Typical large scale runs with over 100 million volumes required about a

day for accomplishing few steady runs and few to several days for accomplishing unsteady runs. The year 2019 is expected to be dominated by unsteady simulations of higher fidelity requiring several days of computational effort with about 10000 cores; in case of availability, these problems can engage the full Cray machine for few days.

5.54 million CPU core hours of SahasraT were used.

3.1.1.4 Publications

1. Praveen Kumar B., N. Balakrishnan, Prediction of Longitudinal Dynamic Derivatives for TransCruiser Aircraft from Unsteady RANS Computations, Symposium on Applied Aerodynamics and Design of Aerospace Vehicles, 28 November – 1 December, 2018, Royal Orchid Resort & Convention Center, Bangalore, India.

2. Navneet A Gopinath, Munikrishna N, Nikhil V Shende, N. Balakrishnan, High lift JAXA Standard Model (JSM) flow prediction using CFD solver HiFUN, Symposium on Applied Aerodynamics and Design of Aerospace Vehicles, 28 November – 1 December, 2018, Royal Orchid Resort & Convention Center, Bangalore, India.

3. Mohamed Yousuf, N. Balakrishnan, Residual based mesh adaptation for Meshless LSFD-U solver, AIAA Journal, https://doi.org/10.2514/1.J057633.

3.1.2 Prof. Sourabh Suhas Diwan's Lab

Team: Transition and Turbulence Research Group

3.1.2.1 Research

Entrainment in Steady and Transient Free Shear Flows & Transition in a Laminar Separation Bubble

(a) A study seeking entrainment behavior of free shear flows such as a jet or plume and the effect of heat addition has been conducted. A large part of the computation was utilized towards choosing and implementing appropriate open boundary conditions in the code. Figure 1 shows a cross-section of established jet simulation with instantaneous surface streamlines and passive scalar concentration distribution

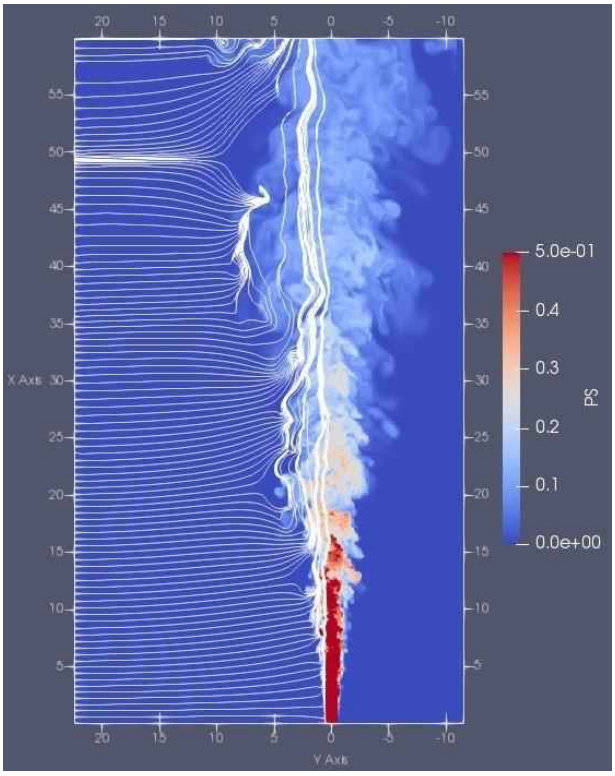

(b) Study of intermittency & turbulent spots in separated shear layer and their comparison with those in an attached boundary layer is being pursued. Figure 2 depicts simulation of an adverse pressure gradient flow over a flat plate, resulting in a laminar separation bubble.

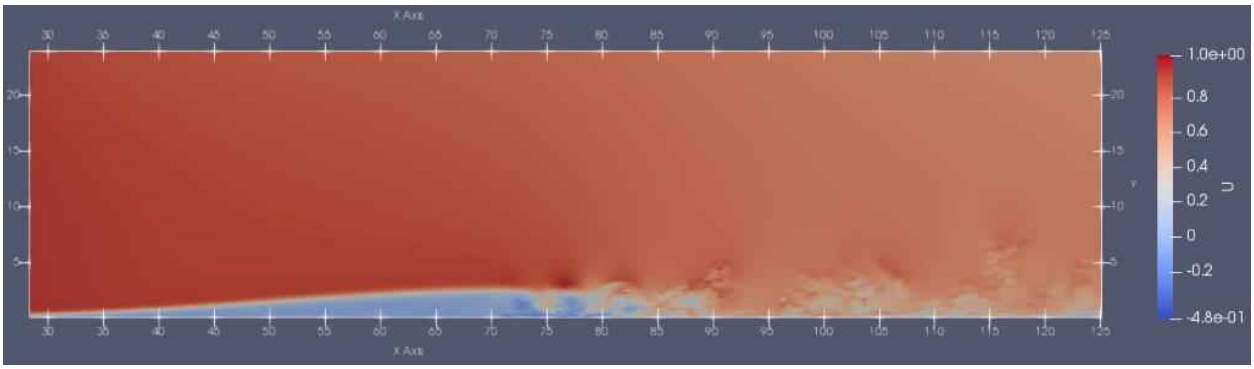

3.1.2.2 SERC Resources and Experiments

3.78 million hours of SahasraT were used.

3.1.2.3 Parallelization

An Incompressible code parallelized using MPI, with fftw used for Poisson solver and is in the process to incorporate pencil fast Fourier transform.

3.1.2.4 Performance

Turbulent jet flows were simulated using 2916 cores (122 nodes) of Cray XC40. No machine available in lab for comparison.

3.2 Centre for Atmospheric and Oceanic Sciences (CAOS)

3.2.1 Prof. Arindam Chakraborty's Lab

3.2.1.1 Research

1. To study about the mechanism of Indian summer monsoon onset, CESM model V1.2.2 is utilized. These simulations are intended to aid observational studies performed using reanalysis datasets.
2. Indian monsoon and its variability under different orbital configurations.

Below is a plot showing average precipitation for the months from March to October from one of the simulations.

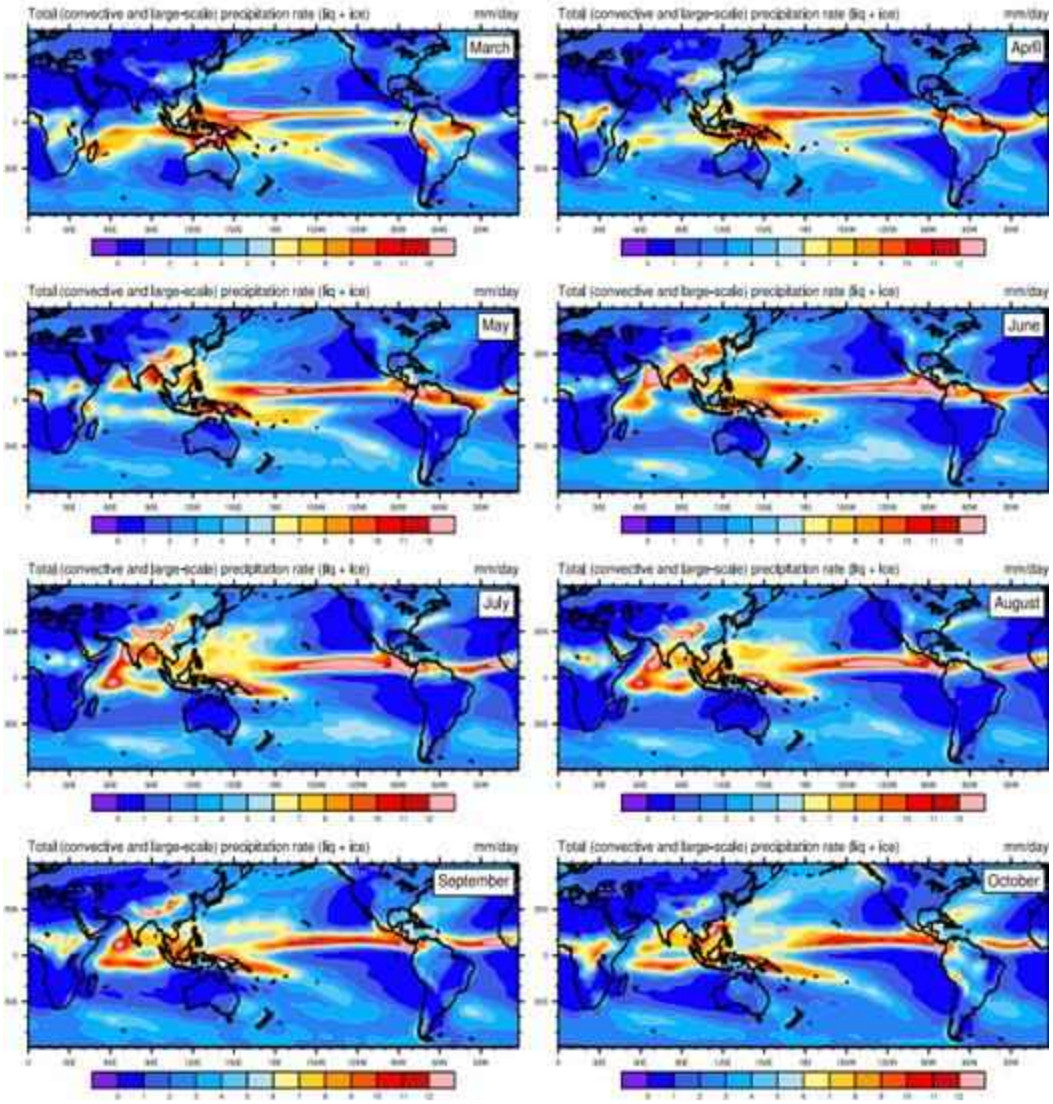

Paleoclimate studies: Understanding the precession of the earth on monsoon climate

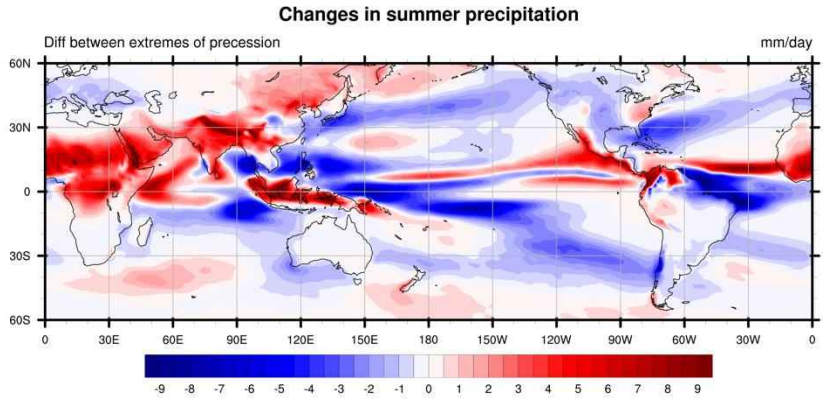

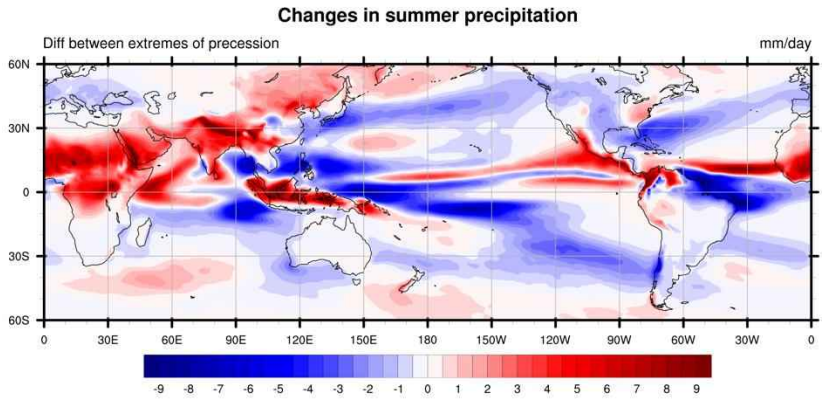

3.2.1.2 SERC Resources and Experiments

Cray SahasraT system was used. Typical number of processors used: 288 for problem #1 and about 1152 cores for problem #2. The model (CESM) is parallelized using MPI. Both the problems use this model. About 1.82 million core hours of SahasraT were used.

3.2.1.3 Performance

Typical execution times vary from 3 to 10 days depending on model configuration. Practically impossible to run on local PC.

3.2.2 Prof. G.S. Bhat's Lab

Student: Jayesh Phadtare.

3.2.2.1 Research

Simulating the Chennai extreme rainfall of 1 December 2015

Weather Research and Forecasting (WRF) model was used to simulate the Chennai extreme rainfall event of 1 December 2015 which lead to the death of around 250 people. Simulations were useful in understanding the functioning of the weather model. This research is a part of the PhD thesis.

3.2.2.2 SERC Resources and Experiments

Tyrone cluster was used. Open Multi-Processing is built in the model itself.

3.3 Centre for Brain Research (CBR)

3.3.1 Prof. Bratati Kahali's Lab

Team: Dr. Bratati Kahali, Krithika Subramanian, Abhishek Panda

3.3.1.1 Research

Human Whole Genome Sequencing (WGS) Data Analysis

Compute Setup: 576 cores of Sahasrat Cray XC40 were used for this experiment. The jobs were submitted in queues upon 24 nodes; each node utilizing 24 cores. MPI based parallel codes in python were written which helped in processing 24 samples in parallel upon 24 compute nodes. Sambamba, BWA, GATK are the major software used to carry out diverse modules in the entire WGS data analysis structure like Sorting, Alignment, Variant Calling of base calls and read pairs from WGS. The mentioned software modules were executed in a multi-core fashion within the nodes using the internal threads option of respective software.

Important results The human genome has 23 pairs of chromosomes. Out of the 23 pairs of chromosomes we have given the alignment quality for Chromosome 2, X and Y in the below figures for 24 samples altogether.

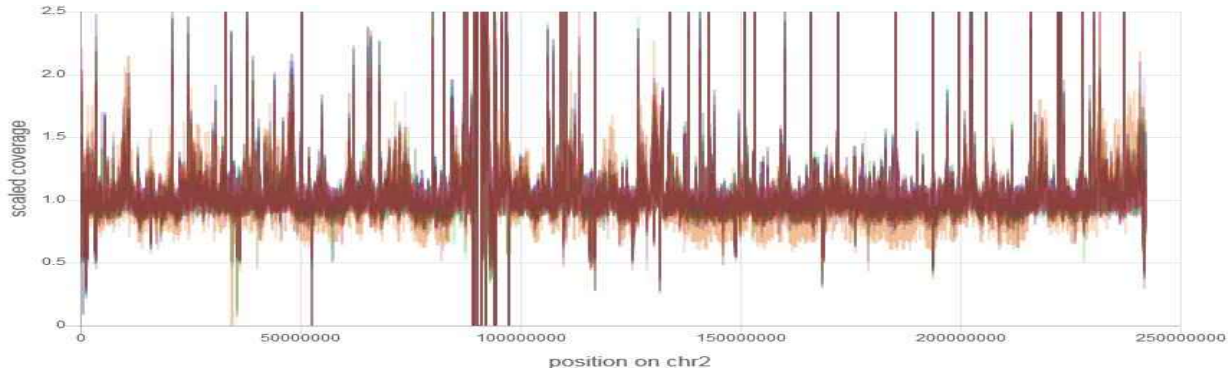

Figure 1: Chromosome 2 has the length of ~242 million base pairs. It is the largest human chromosome and for all the 24 samples the entire region substantially aligned to the human reference genome.

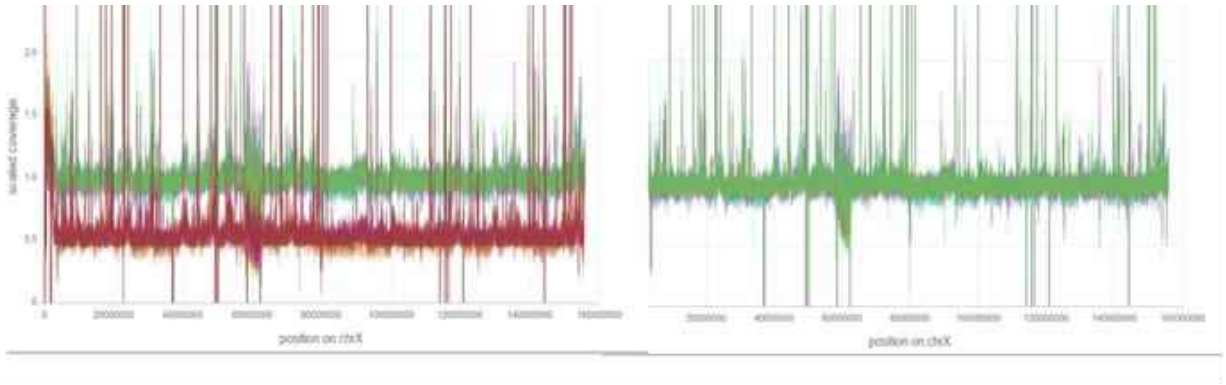

Figure 2: How does **chromosome X** look in whole genome sequencing data? In the left graph, female samples (green) have double the coverage than male samples (Red), overall 24 samples are shown above. The right graph represents only 11 female samples out of the 24 samples. We see this distinctive pattern because females are XX and males are XY in terms of sex chromosomes.

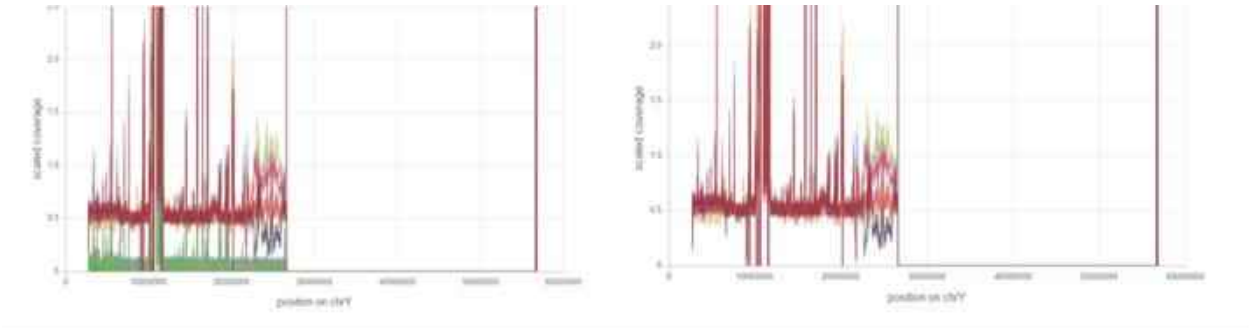

Figure3: How does chromosome Y look in whole genome sequencing data? Both the graphs represent Chromosome Y's scaled coverage among the 24 samples. In the left graph, male samples (red) have double the coverage than female samples(green). The right graph represents 13 male samples out of 24 samples. We see this distinctive pattern because females are XX and males are XY in terms of sex chromosomes.

3.3.1.2 SERC Resources and Experiments

SahasraT Usage: 27648 core hours.

3.3.1.3 Performance

The total input size of 24 samples is 2.5TB. The total output size of the entire WGS pipeline for the 24 samples is 68TB. With the increase in number of samples, the storage requirements will increase exponentially, and computational requirements become more complex. The maximum utilization of memory per node is 96 GB, the maximum total memory required for processing just 24 human samples is 2.3 TB for WGS data analysis pipeline. Utilizing 24 nodes in parallel in Sahasrat helped in completing the WGS data analysis of 24 samples within a total time of 48hours. The maximum wall-time was 12 hours for each step of the pipeline jobs. Each step in our pipeline has different completion time depending upon the nature of job, but each job got completed within the max walltime allocated i.e., 12 hours.

3.4 Department of Computational and Data Sciences (CDS)

3.4.1 Prof. Debnath Pal's Lab

3.4.1.1 Research

The lab used molecular dynamics (MD) approach to understand the role of kinase activator on AMPK protein kinase and its mutant in breast cancer at structural and functional level. AMPK is a large hetrotrimer protein, comprising of α, β and γ subunits. It contains ~9000 atoms and ~190000 water molecules after MD input preparation for GROMACS based molecular dynamics.

3.4.1.2 SERC Resources and Experiments

240-480 CPUs cores of Cray SahasraT were used for GROMACS based molecular dynamics. Also, 12-108 GPUs CUDA cores were used for initial run. For test run, 32 to 256 cores of Tyrone HPC were used for test runs. GROMACS used MPI and OpenMP parallelization strategies.

1.31 million core hours of SahasraT were used.

3.4.1.3 Performance

With the CPUs, performance of ~30 ns/day was obtained. With GPUs, the performance was not good. Hence, completely shifted to CPUs run.

In lab's system with AMD Phenom (tm) II X6 1100T Processor (6 CPU cores), Geforce-gtx-1050-ti 4GB (768 CUDA cores), and 16 GB RAM, performance achieved around 3ns/day.

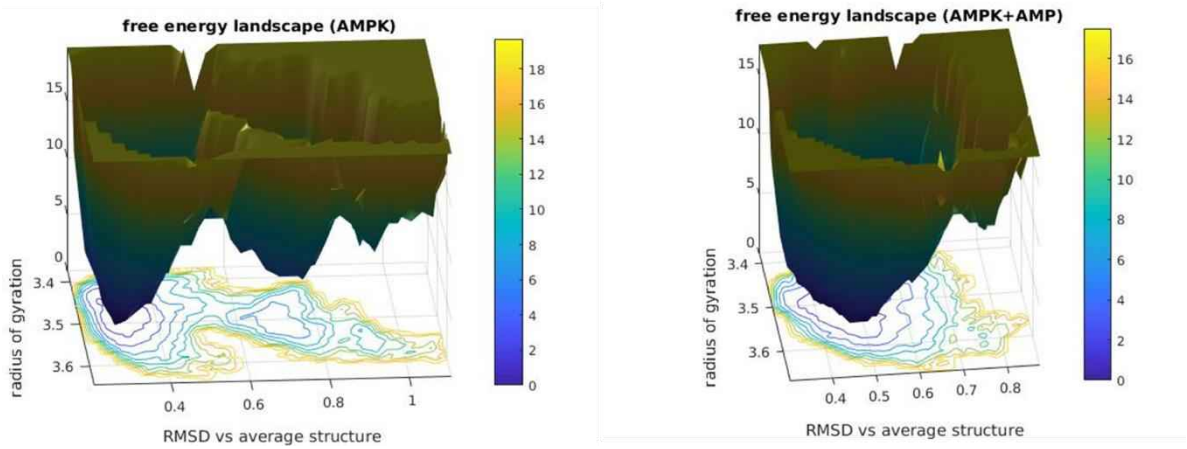

Figure showing Gibbs free energy landscapes AMPK and AMP-AMPK bound states using MD run

3.4.2 Prof. Sashikumaar Ganesan's Lab

Team: Neha Iyer and Sashikumaar Ganesan, Computational Mathematics Group, CDS, IISc

3.4.2.1 Research

Discretization of partial differential equations (PDEs) arising in large scale problems using finite element method (FEM) results in a huge system (order of millions) of algebraic equations. To solve the system, we use the parallel finite element package ParMooN, where the mesh is partitioned among multiple MPI processes using Metis. Each process classifies its degrees of freedoms (DOFs, the unknown solution coefficients) into different types *(independent, dependent and halo)* based on the DOF's connectivity with the neighboring process.

Objective: Development of MPI + OpenMP + CUDA parallel algorithms for iterative solvers such as Jacobi and SOR used in geometric multigrid cycles implemented in ParMooN and to study the performance of the parallel algorithms in following scenarios:

a. Smoothing iterations performed on GPU for all types of degrees of freedom (DOFs)
b. Overlapping smoothing iterations on GPU and host for different types of DOFs
c. Smoothing iterations performed on GPU for all types of (DOFs) for levels above a threshold and performed on host for levels below the threshold and vice versa.

3.4.2.2 SERC Resources and Experiments

a. CPU only cluster: Upto 100 nodes with 24 CPU cores per node
b. Accelerator Nvidia GPU cluster: Upto 16 nodes with 8 CPU cores per node

330113 core hours of SahasraT were used.

3.4.2.3 Parallelization

a. Idea is to perform smoothing iterations of a certain type of DOFs on GPU at the same time perform smoothing iterations for other type of DOFs on host CPU in order to utilize both GPU and CPU

resources simultaneously by leveraging upon the asynchronous nature of CUDA API calls and CUDA streams.

b. OpenMP for loop parallelization is also employed in the smoothing iteration step and DOF coloring step so that DOFs of the same color can be processed in parallel.
c. CUDA Multi-Process service (MPS) is used to enable concurrent execution of kernel and memcopy operations from different MPI processes on the same GPU device on a node.

3.4.2.4 Performance

a. Typical execution times in Sahasrat supercomputer cluster is on an average 100~200 secs for order of million DOFs depending on number of MPI processes.
b. On local lab system Intel Core i7 equipped with one NVIDIA GPU accelerator 1080Ti **only upto 6 MPI processes can be executed in parallel** due to GPU memory constraints.
c. On **Sahasrat upto 24 GPU nodes could be utilized each node with 12 CPU cores.**

Total MPI processes	Total runtime in Local system (sec.)	Total runtime in Sahasrat (sec.)
2	326.49	503.14
4	234.13	289.38
6	299.14	221.53
8	-	169.29
16	-	113.66
36	-	77.11

3.4.3 Prof. Sathish Vadhiyar's Lab

Team: Rintu Panja, Soham Halder

SahasraT usage: 200318 core hours.

3.4.3.1 Research

Efficient processing of large-scale graph applications on heterogeneous CPU-GPU systems require effectively harnessing the combined power of both the CPU and GPU devices. Finding minimum spanning tree (MST) is an important graph application and is used in different domains. In this research, the lab proposed a multi-node multi-device algorithm for MST that uses a divide-and-conquer approach by partitioning the input graph across multiple nodes and devices and performing independent Boruvka's MST computations on the devices. The results from the different nodes are merged using a novel hybrid merging algorithm that ensures that the combined results on a node never exceeds the memory capacity of a single npde. The algorithm also simultaneously harnesses both CPU and GPU devices.

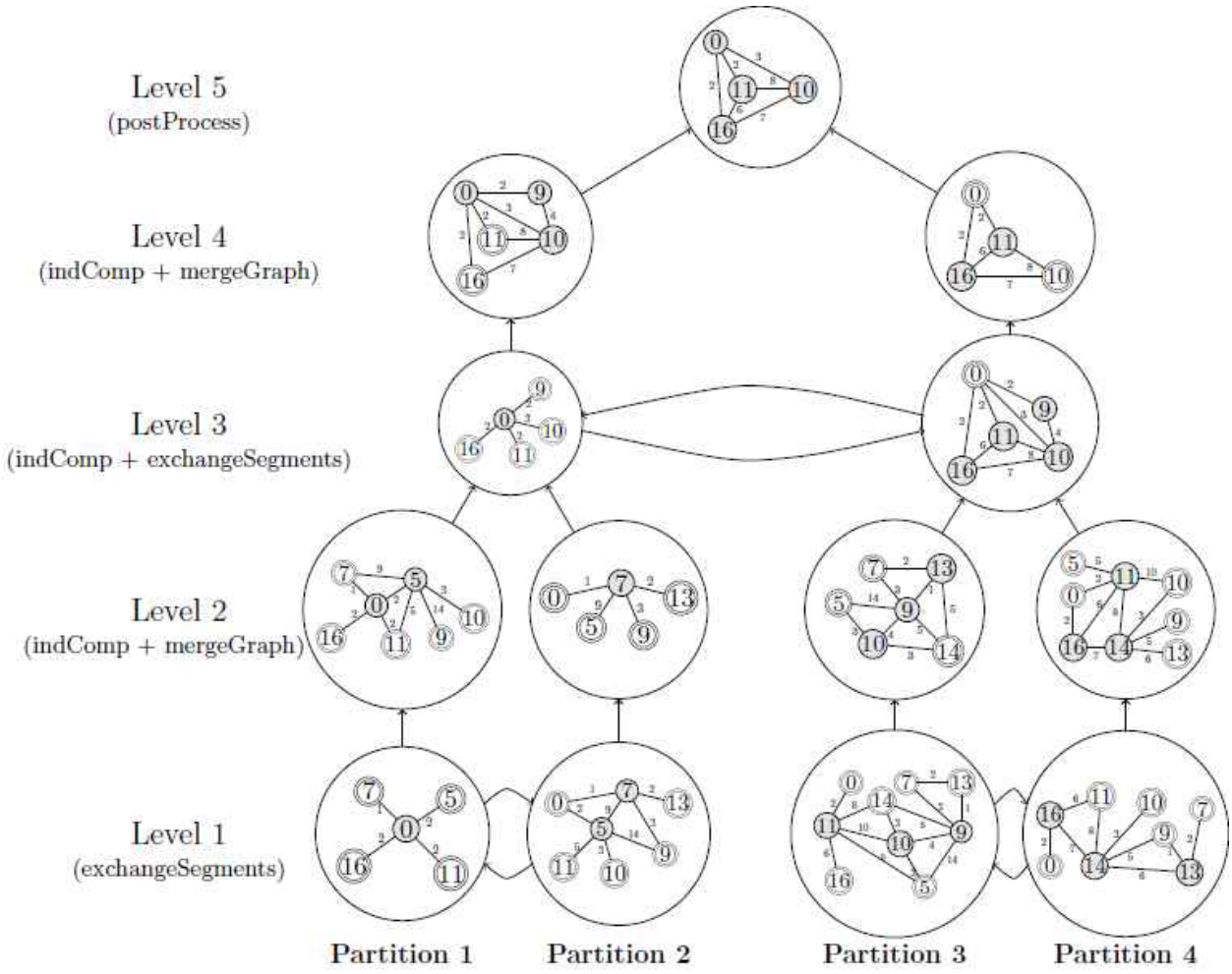

Illustration of Multi-Node Multi-Device MST Algorithm

In another research, the lab built performance models to predict weak scaling of scientific applications using small-scale runs. The challenge was to capture scalability bottlenecks that manifest only at large scale.

3.4.3.2 SERC Resources and Experiments

For the multi-node multi-GPU MST work, up to 16 GPU nodes of SahasraT were used. harnessing the combined power of CPU and GPU on all the nodes. All the graphs used were large-sized graphs with billions of edges that cannot be accommodated in a single node.

For scalability predictions, up to 16K cores of SahasraT were used. Scalability predictions were made for LAMMPS and SMG applications.

3.4.3.3 Performance

The experiments showed that the proposed multi-node multi-GPU MST algorithm shows 24-88% performance improvements over an existing BSP approach. We also show that the algorithm exhibits almost linear scalability for large size graphs that cannot be accommodated in a single machine, and that the use of GPUs result in up to 23% improvement in performance over multi-node CPU-only performance. Our lab GPU node cannot be used for exploring large-size graphs. This could be done only on SahasraT.

The scalability prediction mechanism was able to capture well the scalability trends of large-scale applications.

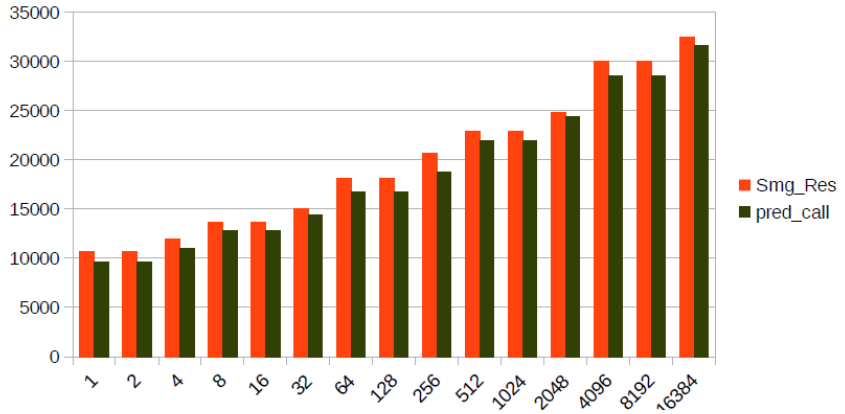

3.4.3.4 Publications

Rintu Panja, Sathish Vadhiyar. **A Multi-Node Multi-Device Parallel Boruvka's MST Algorithm**. In the proceedings of the *International Conference on Parallel Processing (ICPP)*, August 2018, Eugene, USA.

3.5 Department of Chemical Engineering (CE)

3.5.1 Prof. Ganapathy Ayyappa's Lab

Research in our group is focused on understanding molecular and physicochemical properties of membranes and membrane-protein complexes associated with pore forming proteins and G protein-coupled receptors (GPCRs). Using a combination of molecular dynamics simulations, kinetic models and experimental methods we explore kinetics of protein assembly and lipid dynamics on phospholipid membrane and vesicles. These systems are computationally demanding and the HPC resources at SERC have been used extensively in our investigations.

Recent research in collaboration with the Roy laboratory in Chemical Engineering illustrates the role of cholesterol during pore formation by the protein Cytolysin A expressed by the E Coli [***Proceedings of the National Academy of Sciences*** 115, E7323-E7330 (2018)]. In collaboration with Prabal Maiti (Department of Physics) we have recently illustrated a novel pore blocking mechanism which has the potential to develop a strategy to prevent bacterial infections [***Nanoscale,* 8**, 13045-13058 (2016)]. Both these studies have attracted extensive press coverage.

In other works, we are interested in dynamics and binding of small molecules confined in nanopores which have implications in designing nanofluidic devices, understanding transport at the nanoscale and designing materials for gas storage and carbon-dioxide capture. We are currently studying the translational and rotational dynamics of water confined in graphene-oxide membranes with implications for desalination and water purification.

3.5.2 Prof. Prabhu Nott's Lab

3.5.2.1 Research

Granular materials are widely encountered in nature (sand, food grains) and industry (food and pharmaceutical powders, mineral ores), yet their mechanics is poorly understood. We have used a

computational tool called discrete element method (DEM) to obtain a fundamental understanding of the flow in dry grains, and discovered a fundamental phenomenon in sheared granular systems.

3.5.2.2 SERC Resources and Experiments

The idqueue, small and medium jobs were executed in SahasraT.

1.21 million CPU core hours of SahasraT were used.

3.5.2.3 Parallelization

We implement our simulations using LAMMPS (a module on the Sahasrat machine) that uses MPI to parallelize the code.

3.5.2.4 Performance

A 240 cores, 1-hour job on Sahasrat would take 48 hours on a desktop machine (serially) and 12 hours on a local cluster.

3.5.2.5 Industry impact

Our results have helped us advise Hindustan Unilever on the flowability of their processed food powders.

3.6 Centre for Earth Sciences (CEaS)

3.6.1 Dr Attreyee Ghosh's Lab

3.6.1.1 Research

The lab is investigating the causes behind the survival of cratons, the oldest parts of the planet. These regions have survived for billions of years as opposed to other parts of the Earth that gets destroyed within a few million years. The reasons for their survival are still unknown and in this project, with the help of numerical modeling, the lab is exploring some of the physical parameters that might have enabled these cratons to survive for such a long time.

Video: https://www.youtube.com/playlist?list=UUBruY_7eCEfVjnlriZJGdqw

3.6.1.2 SERC Resources and Experiments

Tyrone cluster, maximum cores used: 512. An open access community code that is already parallelized is used.

3.6.1.3 Publications

Traction and strain rate at the base of the lithosphere: An insight into cratonic survival. J. Paul, A. Ghosh, C. Conrad. Geophysical Journal International, in Review.

3.7 Department of Computer Science and Automation (CSA)

3.7.1 Prof. Shalabh Bhatnagar

3.7.1.1 Research

Inherent sequential nature of the First Order Bayesian Optimization (FOBO) methods and the problem of noisy gradient information exacerbates the computational overhead as well as the underlying parameter

estimation problem, limiting their wide applicability. To alleviate this, we developed a parallelizable novel FOBO methods that search for global optima effectively.

3.7.1.2 SERC Resources and Experiments

We used ~30000 cores of CPU only cluster

SahasraT usage: 5.55 million CPU core hours.

3.7.1.3 Parallelization

Most of our tasks run independently, groups of 10-25 processes co-ordinate among themselves using MPC interface.

3.7.1.4 Performance

Our experiments would have taken 6 months on lab systems, whereas we could run them on Sahasrat in 3 days.

3.8 Department of Electronic Systems Engineering (DESE)

3.8.1 Prof. Santanu Mahapatra's Lab

3.8.1.1 Research

Two-dimensional materials are promising candidates for lithium ion battery anodes due to their large surface to volume ratio. The distorted T′ phase of the rhenium disulfide crystal makes the study of lithium binding more complex than for other two-dimensional materials with symmetric crystal structures. We have explored the lithium ion storage capacity of monolayer rhenium disulfide by first-principles based calculations. We've employed hardware-accelerator-assisted high-throughput calculations, using a van der Waals density-functional-theory based 'structure search' technique, to emulate the lithiation process. Exploring 2000 structures, each containing 49 to 98 atoms, we've found the most stable lithiated structures for various lithium concentrations. We've then designed a delithiation algorithm and applied it to those lithiated structures for the estimation of the reversible specific capacity. Despite possessing high molar mass, a reasonably high specific capacity (214.13 mAh/g) and open-circuit voltage (0.8 V), in agreement with experimental results, make rhenium disulfide a promising alternative anode material.

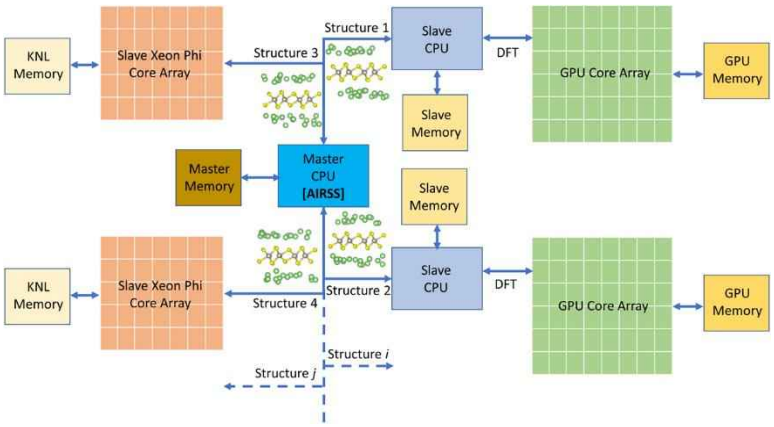

Video:

https://static-content.springer.com/esm/art%3A10.1038%2Fs42004-018-0082-3/MediaObjects/42004_2018_82_MOESM3_ESM.mp4

3.8.1.2 SERC Resources and Experiments

To optimize each structure 4 GPU nodes consisting 4 GPUs and 4 CPU cores or 4 KNL nodes consisting 256 KNL cores have been utilized. In addition to this, 240 CPU cores (10 nodes) were used for some static energy calculations.

3.8.1.3 Parallelization

In this work we've used a master-slave architecture where the Dell Visualization Servers were used as the master nodes to execute the ab-initio random structure searching (AIRSS) and the hardware accelerator-based nodes, namely, Intel Xeon-Phi KNL nodes and NVIDIA K40 GPUs were used as the slaves to perform the density functional theory (DFT) based structure optimizations parallelly. Also, the GPU and KNL codes have been fully optimized for their respective architecture to take advantage of the highly parallel nature of these hardware accelerators.

3.8.1.4 Performance

Depending on the number of atoms and type of species in the structures, each structure took 1.5-4.5 hours to get fully optimized in SERC's hardware accelerator-based clusters. In stark contrast, our lab's latest Broadwell based CPU only cluster with 60 cores takes days to optimize one such structure.

3.8.1.5 Publications

Arnab Kabiraj and Santanu Mahapatra, "High-throughput first-principles-calculations based estimation of lithium ion storage in monolayer rhenium disulfide" Communications Chemistry, Nature Publishing Group (NPG), 2018.

3.9 Inorganic and Physical Chemistry (IPC)

3.9.1 Prof. E.D. Jemmis' Lab

3.9.1.1 Research

1. Hydrogen-Bond is well-known. The lab and others have studied other weak intractions involving the main group elements such as the Halogen-Bond. We thought that this type of weak interactions may exist among the transition metals. To our surprise, none was noticed if we restrict to 18 electron complexes involving non-d10 metals. This study led to the design of new ligands for the purpose and to many consequences of the sigma-hole. (ref.1-3).

2. Boron equivalent of graphene is generated experimentally during the last two years. These 2D-sheets consists of triangles largely, but depending on the metal-template there are varrying number of hexagonal holes. The lab has provided an explanation for the hole-density. This also led to the study of borospherenes (fullerenes involving boron) with large holes. In an independent study we showed that beta-boron (and not tau-boron) is the most stable allotrope of boron. (ref.4-7).

3. Transition metals change the reactivity patterns of carbon and boron. The lab has studied the coupling reactions of boron with itself under the influence of transtion metals and designed ways to make the boron mimic reactions of carbon. (ref.8-9).

4. Carbon Nanothreads is an emerging area in nanochemistry and materials. The lab studied the ways to design admantane-based nanothreads which have superior mechanical properties. (ref.10).

5. In addition to these we collaborated with experimentalists within the Department and outside the Institute on (a) a model for V2O5-based enzymes (nanoisozymes) with G. Mukesh (ref.11), (b) on sigma-complexes of transition metals with Balaji Jagirdar (ref.12), (c) on controlling Lewis acity of Bi complexes using ligand bite angle with Ajay Venugopal (IISERTVM) (ref.13), and (d) on elucidating the structure of metallaboranes with Sundar Ghosh (IITM) (ref.14).

3.9.1.2 SERC Resources and Experiments

Solid state calculations have been done using VASP, installed in SAHASRAT. The number of node count varies from 5 to 20. Parallelization strategy is used to enhance the performance of the code. Most of the jobs generally take two to three days to complete, as the number of atoms in most of the cases is more than 100.

1.26 million core hours of SahasraT were used.

The lab has used Gaussian 09 program package installed in dell, delta and tyrone clusters for molecular electronic structure calculation. The structural optimization and electronic structure calculations are done to understand the stability of different structures. The intermediate and transition state calculations are also performed. The number of nodes used for the calculations were 1-4 and number of processors used were 16-256 as given in SERC site.

Total CPU time: Tyrone cluster- 42183711, Delta cluster- 20859156, Dell-78559491.

3.9.1.3 Performance

Particularly, tyrone cluster with 256 core and delta cluster with 32 core are found to be quite faster than the ipc-cluster with 8 processors (max. limit).

3.9.1.4 Publications

1. Jyothish Joy, Eluvathingal D. Jemmis, Contrasting Behavior of the Z-Bonds in X-Z···Y Weak Interactions: Z = Main Group Elements Versus the Transition Metals, Inorg. Chem. 56, 1132-1143 (2017).

2. Jyothish Joy, Eluvathingal D. Jemmis, A Halogen Bond Route to Shorten the Ultrashort Sextuple Bond in Cr_2 and Mo_2, Chem. Commun. 53, 8168-8171 (2017).

3. Joy Jyothish, E. Akhil and E. D. Jemmis, Halogen bond shortens and strengthens the bridge bond of [1.1.1]propellane and the open form of [2.2.2]propellane. Phys. Chem. Chem. Phys., DOI: 10.1039/c8cp05125a (2018).

4. Naiwrit Karmodak, Eluvathingal D. Jemmis, Role of Holes in borophenes: an ab-initio study of the structure and stability with and without metal template, Angew. Chem. 56, 10093-10097 (2017).

5. Naiwrit Karmodak, E. D. Jemmis, Metal Templates and Boron Sources Controlling Borophene Structures: An Ab Initio Study, J. Phys. Chem. C, 122, 2268-2274 (2018).

6. Naiwrit Karmodak, Eluvathingal D. Jemmis, Dynamic behavior of the exohedral transition metal complexes of B_{40}: eta6- and eta7-$B_{40}Cr(CO)_3$ and $Cr(CO)_3$-eta7-B_{40}-eta7-$Cr(CO)_3$, J. Chem. Sci. 129, 1061-1067 (2017).

7. Naiwrit Karmodak, Eluvathingal D. Jemmis, Fragment approach to the electronic structure of tau-boron allotrope, Phys. Rev. B, 95, 165128 (2017).

8. Sagar Ghorai, Eluvathingal D. Jemmis, A DFT study of the stabilization of B-B triple bond in a metallaborocycle: Contrasting electronic structures of boron and carbon analogs, Chem. Eur. J. 23, 9746-9751 (2017).

9. Sagar Ghorai, E. D. Jemmis, B-B coupling and B-B catenation: Computational study of the structure and reactions of metal-bis(borylene) complexes. Chem. Eur. J., DOI: 10.1002/chem.201804599 (2018).

10. S. Marutheeswaran and E. D. Jemmis, Adamantane-Derived Carbon Nanothreads: High Structural Stability and Mechanical Strength, J. Phys. Chem. C, 2018, 122 (14), pp 7945-7950.

11. Sourav Ghosh, Punarbasu Roy, Naiwrit Karmodak, E. D. Jemmis, Govindasamy Mugesh, Nanoisozymes: Crystal Facet-Dependent Enzyme Mimetic Activity of V2O5 Nanomaterials, Angew. Chem. Int.Ed. 130, 4600-4605 (2018).

12. A. Ramaraj, K. Hari Krishna Reddy, Helena Keil, Dietmar Stalke, Eluvathingal D. Jemmis, and Balaji R. Jagirdar, Approaches to Sigma-complexes via Displacement of Agostic Interactions: an Experimental and Theoretical Investigation, Organometallics, 36, 2736-2745 (2017). Shyama Ramakrishnan, E. D. Jemmis, Origin of beta-agostic interaction in d0-transition metal alkyl complexes: Influence of ligands, J. Organomet. Chem., 865, 37-44 (2018).

13. Ramkumar Kannan, Sandeep Kumar, Alex Andrews, Eluvathingal D. Jemmis, and Ajay Venugopal, Consequence of Ligand Bite Angle on Bismuth Lewis Acidity, Inorg. Chem. 56, 9391-9395 (2017).

14. Bijan Mondal, Ranjit Bag, Sagar Ghorai, K Bakthavachalam, E. D. Jemmis, Sundargopal Ghosh, Synthesis, Structure, Bonding and Reactivity of Metal Complexes comprising Diborane(4) and Diborene(2): [{Cp*Mo(CO)2}2{μ-?n2:n2-B2H4}] and [{Cp*M(CO)2}2B2H2M(CO)4], M=Mo,W. Angew. Chem. Int.Ed. , 57, 8079-8083 (2018).

3.10 Department of Materials Engineering (Mat Eng.)

3.10.1 Prof. Abhik Choudhury's Lab

3.10.1.1Research

1. Microstructure Evolution in Eutectic Solidification

The Sn-Zn eutectic alloy, which is a potential replacement for Pb-based alloys in solder applications, shows a variety of microstructures (structure of material at the micrometre scale) with changing experimental conditions. Through phase-field simulations at the mesoscopic scale, we study the microstructure evolution during directional growth in this alloy. Thus, we obtain the self-organized steady state patterns arising during coupled two-phase growth of experimentally relevant domain sizes under different process conditions as encountered in the actual directional solidification of crystals.

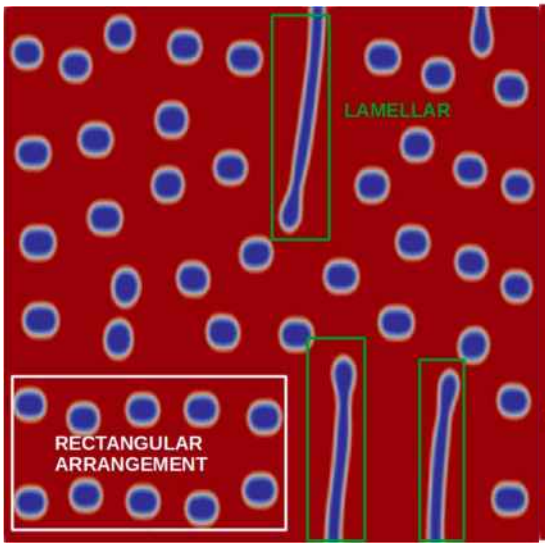

Figure 1: Anisotropic Interfacial Energies

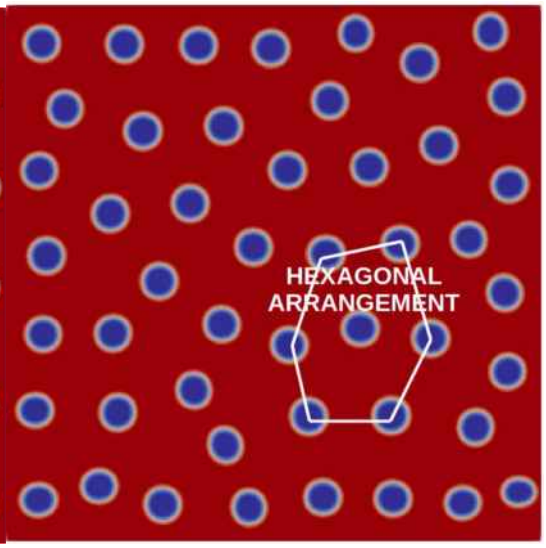

Figure 2: Isotropic Interfacial Energies

https://drive.google.com/open?id=1Rv1PT1kmyjXQ6wwijD4mPTCL3gMTNtgE

Video: Large-scale Microstructure Evolution with anisotropy (left) and isotropy (right)

2. Process-Structure-Property Relationship in Organic Photovoltaics

We have developed a theoretical framework through which one can narrow the multi-parameter window in Organic Photovoltaics (OPV). This is achieved by rst establishing process-structure correlations i.e., generating a range of morphologies with dierent blend ratios and annealing times. Secondly, by developing eective electronic properties of the morphologies which allows one to characterize the performance of each of the obtained morphologies. This will complete the theoretical Process-Structure-Property linkage which will allow the optimization of the process parameters for device applications.

3. Solid-State Phase Transformations

The mechanical properties of the alloys are also dependent on the shapes of the precipitates. Therefore, in order to investigate the mechanical response of a material which undergoes precipitation during heat treatment, it is important to derive the range of precipitate shapes that evolve. In this context, we introduce a novel phase- eld method where we minimize the functional consisting of the elastic and surface energy contributions while preserving the precipitate volume. Using this technique, we reproduce the shape-bifurcation diagrams for the cases of pure dilatational misfit that have been studied previously using sharp interface methods.

Video: https://drive.google.com/open?id=1OM6OtfXjSZUfcEX-oigQZpxWxiDtOMnI

3.10.1.2SERC Resources and Experiments

We consistently use SERC's medium queue with about 2000 processors. Also, we took part in the HPC Grand Challenge Day 2018 and ran simulations on all of SahasraT's 32K processors. For simulating microstructures in OPV, we used CRAY's GPU nodes. Each simulation required one GPU node for a total

of 8 days. For the study of equilibrium shape of the precipitates having a domain size 1000*1000, we have utilized the small 72 queue.

1.24 million core hours of SahasraT were used.

3.10.1.3 Parallelization

We implemented MPI based parallelism in the nite dierence phase eld code. Also, we implemented parallel I/O using the Parallel-HDF5 le format. To simulate crystal growth in one direction using a nite domain size, we use a moving window technique to focus on the concerned solid-liquid interfacial area and employ periodical shifts in the entire domain. We implemented the microstructure evolution code in Fourier Space using cuFFT library of Nvidia CUDA C language.

3.10.1.4 Performance

Our large scale simulations of domain size 600X420X420 are only feasible on SahasraT. Had we run the same simulations on our lab clusters with 200 processors, the time taken would be about 9 months. TESLA K40m GPU cards have 2880 cores that are 10 times the no. of cores on our computer and thus gives a speed-up of 8 times.

3.10.1.5 Publications

1. B. Bhadak, R. Sankarasubramanian, A. Choudhury, Metall and Mat Trans A (2018), 49:57055726., Phase eld modeling of equilibrium shapes of the precipitate under infuence of the coherency stresses.
2. S. Khanna, A.S. Kiran, A. Choudhury, Seventh International Conference on Solidi cation Science and Processing (ICSSP-2018).
3. F. Kaka, P.C. Ramamurthy, A. Choudhury, International Conference on Emerging Electronics (ICEE), IEEE-2018.

3.11 Molecular Biophysics Unit (MBU)

3.11.1 Prof. Anand Srivastava's Lab

3.11.1.1 Research

Biological membrane hosts nearly half of a cell's vital functions including vesicular transport, ion signalling etc. These processes are often coupled with large scale conformational changes in proteins and rearrangments in lipids, which occur through several intermediates. The experimental difficulties associated with capturing such short-lived intermediates in protein conformations and membrane topologies point to the requirement for high-fidelity multiscale computational simulations. Currently, we are exploring the molecular mechanisms underlying the dynamin-assisted membrane fission and K2P channel-assisted polymodal ion signalling.

1. Molecular origin of polymodal sensitivity of TREK-1 K2P channel:

TREK-1 K2P ion-channel has a long intrinisically disordered tail at its cytosolic domain (CTD) that recognizes multiple distinct stimuli such as bilayer stretch, pH, temperature, change in membrane lipid composition, second messenger binding etc. We explored the molecular origin of such polymodality utilizing a novel algorithm that combines temperature replica exchange and solute tempering methods. Our simulation reveals that the polymodality has its roots in the ability of the CTD to take up different conformations that are environmentally dependent (Figure 1).

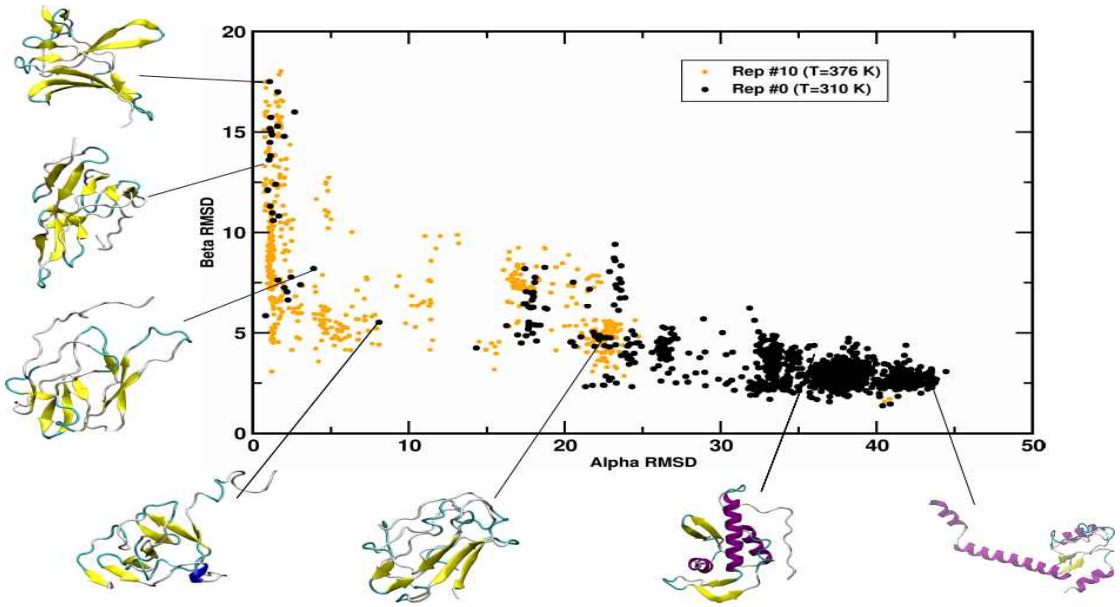

Figure 1: Transient heterogeneous conformations of C-terminal domain that elicit polymodal sensitivity in TREK-1 K2P channel.

2. Flexible pivoting of the PHD in dynamin catalyzes fission by affecting membrane properties

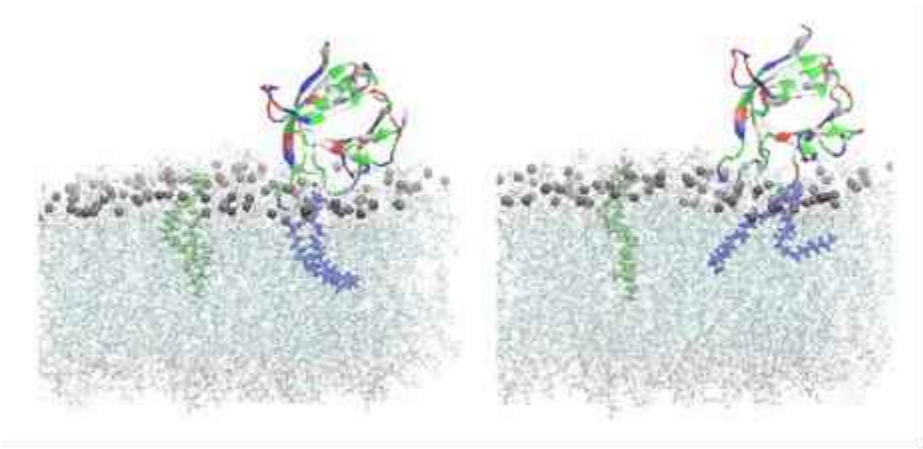

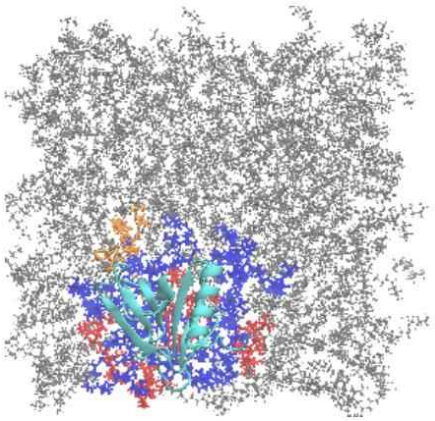

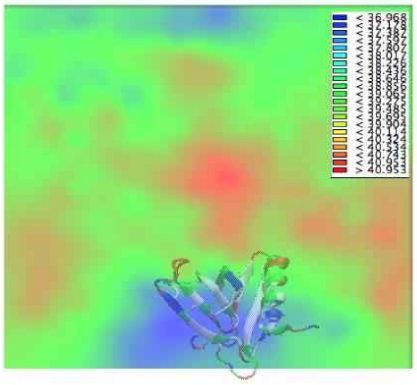

3.11.1.2 SERC Resources and Experiments

We used upto 150 CPU nodes (3600 cores) on CRAY SahasraT. We ran our simulations using Gromacs molecular dynamics package.

SahasraT usage: 4,13 million CPU core hours.

3.11.1.3 Parallelization

The Message Passing Interface (MPI) was implemented using cray-mpich 7.6.0.

3.11.1.4 Performance

In dynamin-mediated membrane fission work for a system comprising of about 200000 atoms, using 42 nodes (1008 cores), we produce ~85 ns/day in Cray XC40. This would otherwise take 5-7 days with resources available in our lab (8nodes with 224 cores).

In the other work we sampled the conformational landscape of K2P channel C-terminal domain, which is computationally very expensive. The use of replica exchange methods, though efficient in exploring the landscape, it required about 25 replicas of a system to be simulated parallelly in different temperature space. Thus a massively parallel environment was necessary for this application and Cray-XC40 is our only option. Using 150 nodes (3600 cores), we were able to generate 35ns/replica/day (840ns in total in a day)

3.11.2 Prof. N Srinivasan's Lab

3.11.2.1 Research

Use of computationally designed artificial protein sequences for the purpose of enabling detection of distant homologues that are often missed out by routine sequence search methods. We have observed that plugging in these protein like designed sequences into the sequence space has narrowed the structure to sequence gap appreciably.

3.11.2.2 SERC Resources and Experiments

Extensively used the Tyrone Cluster and the cray super computing facility. Using a maximum of 264 cores.

SahasraT usage: 831450 CPU core hours.

3.11.2.3 Parallelization

Employed MPI parallel. The software(hmmer) has an inherent cpu thread parallelization option as well.

3.11.2.4 Performance

In comparison to lab systems, very good scaling 0.8 (when using 264 cores).

3.11.2.5 Publications

Kumar Gayatri, Richa Mudgal, Narayanaswamy Srinivasan, and Sankaran Sandhya. "Use of designed sequences in protein structure recognition." Biology direct 13, no. 1 (2018): 8.

3.11.3 Prof. Saraswati Vishveshwara's Lab

3.11.3.1 Research

Molecular Dynamic Simulations of proteins have been done to analyse their conformational space.

The conformations are analysed as protein structure networks, using the method developed in our laboratory. The method NSS (Network Scoring Scheme) compares any two networks based on their graph spectral properties (Journal of Complex Networks, 5(2), pp.219-244. doi.org/10.1093/comnet/cnw016).

The structures obtained along the trajectory of the simulation have been compared against each other in terms of their side chain connectivity, using Network Similarity Score. The following are the details of the SERC facilities utilized.

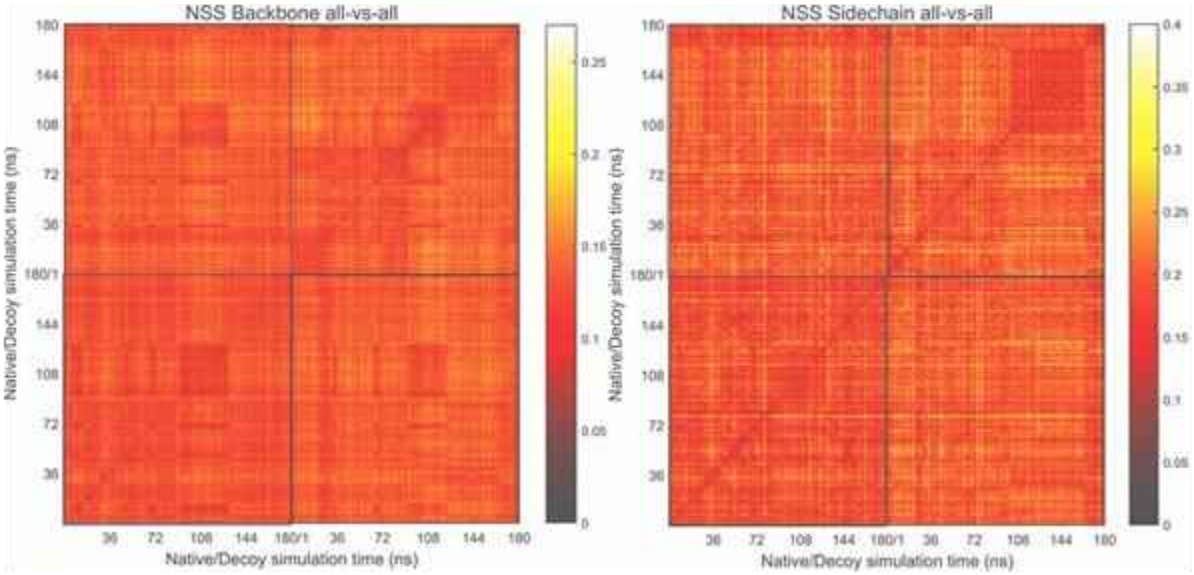

Figure : The 2D-NSS Plot of TR829 Native and Decoy simulation frames for backbone and side-chain. For each of the backbone and side-chain plots: Top left and Bottom right boxes—2D-NSS of TR829 Native frames versus TR829 Decoy frames. Top right box—2D-NSS of TR829 decoy frames only. Bottom left box—2D-NSS of TR829 native frames only. The 2500 frames are used for each system selected at equal intervals of 72 ps over the 180 ns simulation trajectory.

3.11.3.2 SERC Resources and Experiments

Delta Cluster , 64 x 16 cores used.

SahasraT usage: 128689 CPU core hours.

3.11.3.3 Parallelization

Multithreading

3.11.3.4 Performance

We were able to do the analysis in 8 hours which would have taken around 200 hours in our lab system

3.11.3.5 Publications

Journal Proteins:SFB (Ghosh, S., Gadiyaram, V., and Vishveshwara, S.(2017). Validation of Protein Structure Models using Network Similarity Score. Proteins: Structure, Function and Bioinformatics, 85(9) 1759-1776)

3.12 Materials Research Centre (MRC)

3.12.1 Prof. Abhishek Singh's Lab

3.12.1.1 Research

The lab has used SERC HPC facility for computational modelling of materials, especially in applications, where extensive computational resources were required. The main problems solved using this facility includes the prediction models for various physical properties using machine learning, overpotential calculation, calculations for defects study, discovering novel topological materials and determining their exotic topological properties, non-linear polarization, evaluation of the anharmonic contributions to the lattice thermal conductivity of thermoelectric materials, and thermoelectric figure of merit.

One of the biggest challenges was to develop the machine learning models using large datasets, which requires an extensive computational facility. SERC HPC has been very useful for these data-driven methods.

Machine learning model for band-gap prediction

http://anant.mrc.iisc.ac.in/ ***(machine-learning database of MXene)***

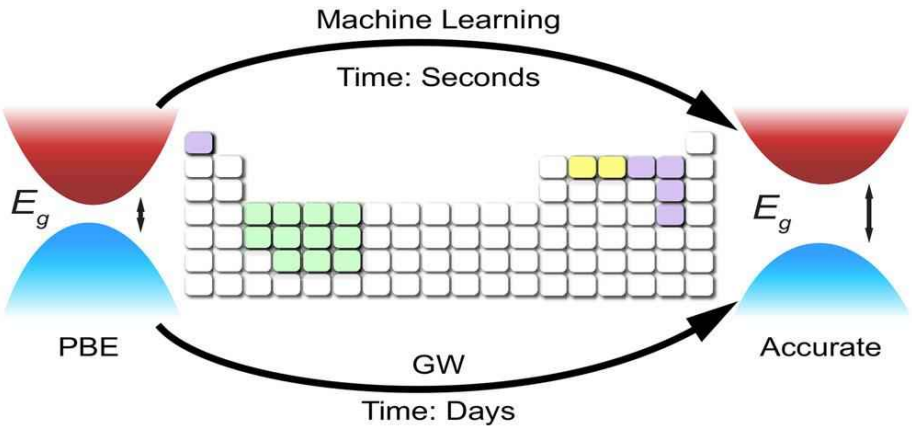

High Thermoelectric Figure of Merit in Ternary Chalcopyrites

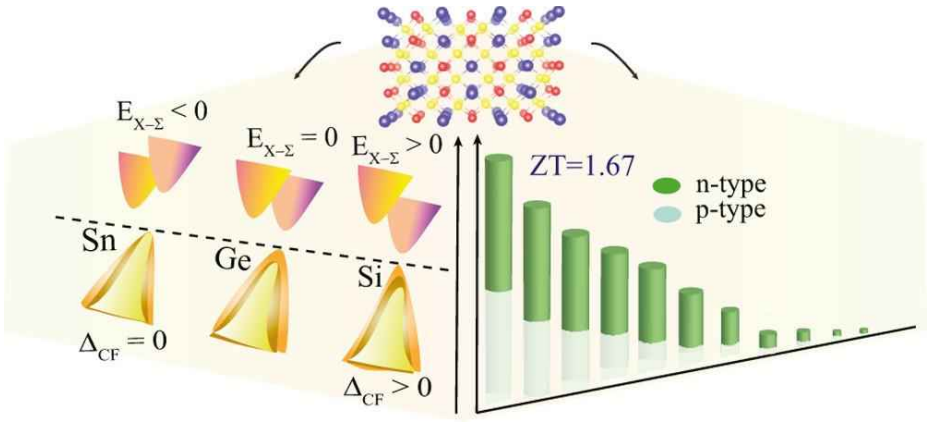

Defect Transition-Levels Engineering

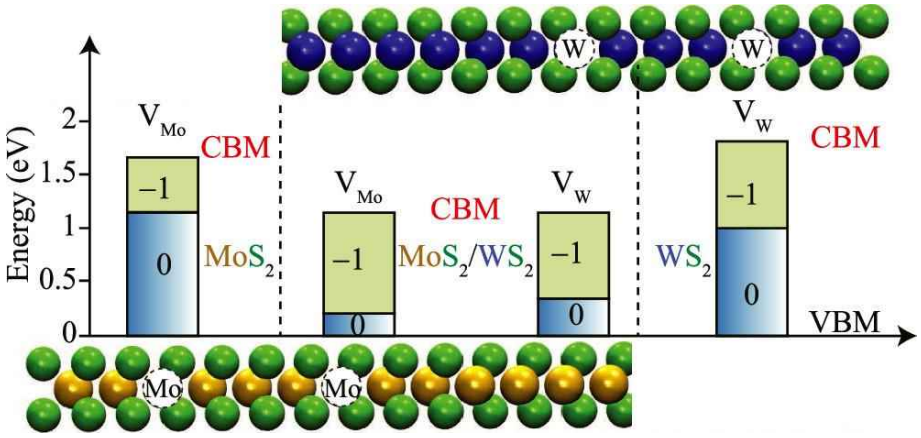

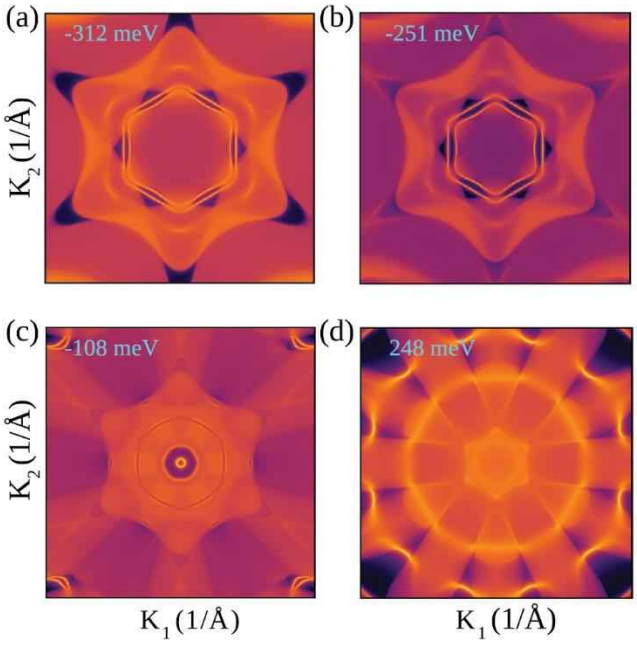

Multiple Triple-Point Fermions in Heusler Compounds

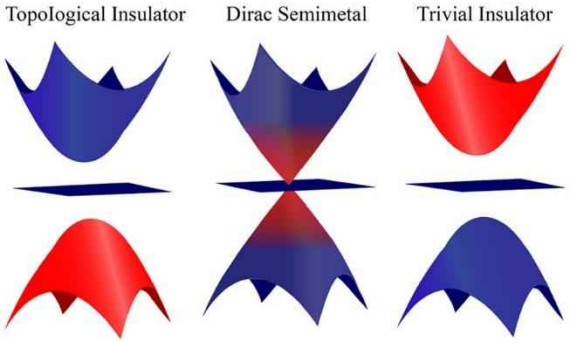

Pressure Induced Topological Phase Transitions

Promising Water Splitting Photocatalyst: C_2N/WS_2 Van der Waals Type-II Heterostructure

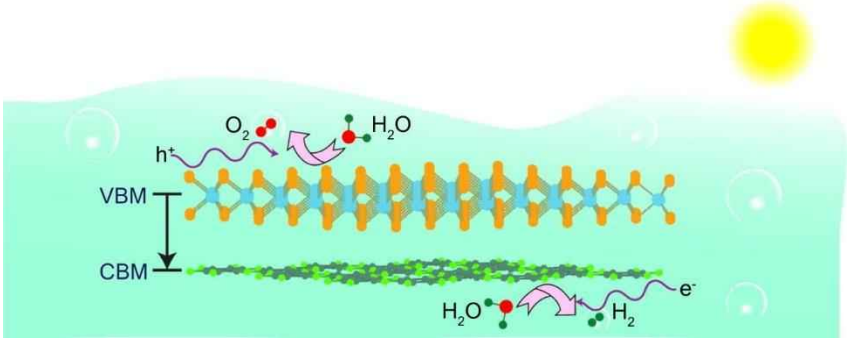

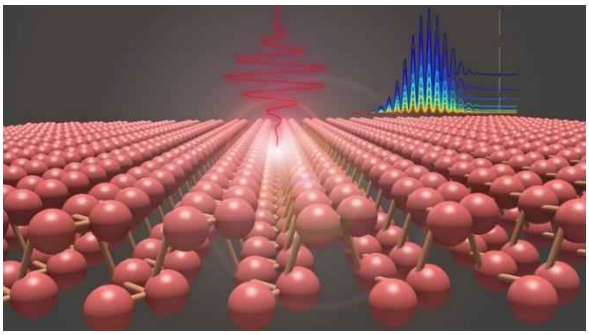

Nonlinear Polarization and Low-Dissipation Ultrafast Optical Switching in Phosphorene

Interplay of Structural and Bonding Characters in Thermal Conductivity

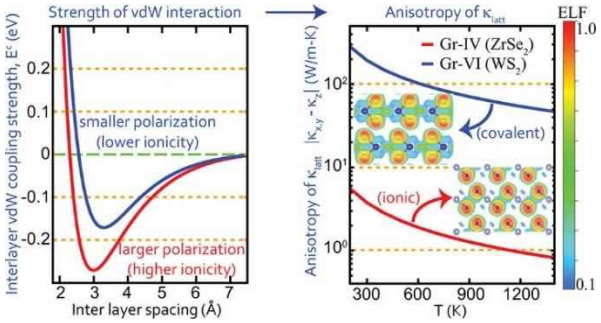

Steps for CO_2 electro-reduction to CH_4

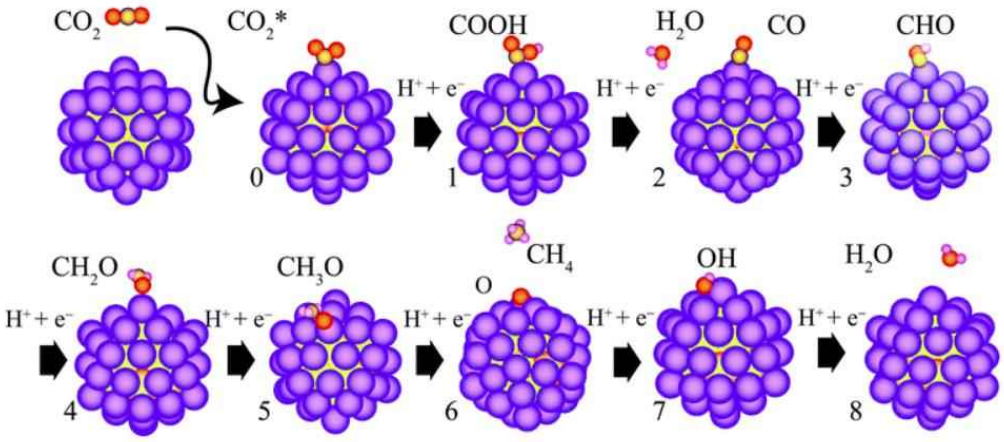

3.12.1.2 SERC Resources and Experiments

In most of the problems, the commonly used HPC resources are debug, small and small72 queue with 240 cores. However, in few cases, we have also utilized medium queue.

A parallel code VASP, Quantum Espresso, WannierTools, ShengBTE were used, with both multicore and multinode parallelization.

6.19 million core hours were used.

3.12.1.3 Performance

The computational facilities at SERC are much faster than our lab cluster. Typical execution times using SERC HPC systems were 24 hours or 72 hours. The same task would have taken at least an order of magnitude more time on the local facility.

3.12.1.4 Publications

1. High Thermoelectric Figure of Merit via Tunable Valley Convergence Coupled Low Thermal Conductivity in $A^{II}B^{IV}C^{V}_2$ Chalcopyrites, M. Mukherjee, G. Yumnam, and Abhishek K. Singh, *J. Phys. Chem. C* 122, 51, 29150 (2018)
2. Amine Functionalized Zirconium Metal-Organic Framework as an Effective Chemiresistive Sensor for Acidic Gases, M. E. DMello, N. Sundaram, A. Singh, Abhishek K. Singh and S. B. Kalidindi, *Chem. Commun.*, 2019,55, 349-352
3. Engineering Defect Transition-Levels through van der Waals Heterostructure, A. Singh, A. Manjanath and Abhishek K. Singh, *J. Phys. Chem. C* 122, 24475 (2018)
4. Synergistic Core-shell Interactions Enable Ultra-low Overpotentials for Enhanced CO_2 Electro-reduction Activity, R. Ahmad and Abhishek K. Singh, *J. Mater. Chem. A* 6, 21120 (2018)
5. Multiple Triple-Point Fermions in Heusler Compounds, R. K. Barik, R. L. Shinde, and Abhishek K. Singh, *J. Phys. Cond. Mat.* 30, 375702 (2018)
6. Nonlinear Polarization and Low-Dissipation Ultrafast Optical Switching in Phosphorene, R. Shinde, and Abhishek K. Singh, *J. Phys. Chem. C* 122, 19146 (2018)
7. Machine-Learning-Assisted Accurate Band Gap Predictions of Functionalized MXene, A. C. Rajan, A. Mishra, S. Satsangi, R. Vaish, H. Mizuseki, K. R. Lee and Abhishek K. Singh, *Chem. Mater.* 30, 4031 (2018)
8. Pressure-Induced Topological Phase Transitions in $CdGeSb_2$ and $CdSnSb_2$, R. Juneja, R. Shinde, and Abhishek K. Singh, *J. Phys. Chem. Lett.* 9, 2202 (2018)
9. Structural, Vibrational, and Electronic Topological Transitions of $Bi_{1.5}Sb_{0.5}Te_{1.8}Se_{1.2}$ under Pressure, J. S. Kim, R. Juneja, N. P. Salke, W. Palosz, V. Swaminathan, S. Trivedi, and Abhishek K. Singh, D. Akinwande and J. Lin, *J. Appl. Phys*. 123, 115903 (2018)
10. Interplay of Structural and Bonding Characters in Thermal Conductivity and Born-Effective Charge of Transition Metal Di chalcogenides, G. Yamnam, T. Pandey, and Abhishek K. Singh, *J. Phys. Chem. C* 122, 2521 (2018)
11. C_2N/WS_2 Van der Waals Type-II Heterostructure as a Promising Water Splitting Photocatalyst, R. Kumar, D. Das, and Abhishek K. Singh, *J. Catal.* 359, 143 (2018)
12. Origami inspired Three-Dimensional Interconnected Molybdenum Carbide Nanoflakes, R. Koizumi, S. Ozden, A. Samanta, A. P. Alves, A. Mishra, G. Ye, G. G. Silva, R. Vajtai, Abhishek K. Singh, C. S. Tiwary, and P. M. Ajayan, *Adv. Mater. Interfaces*, 1701113 (2018)
13. Atomically thin gallium layers from solid-melt exfoliation, V. Kochat*, A. Samanta*, Y. Zhang, S. Bhowmick, P. Manimunda, S. A. S. Asif, A. Stender, R. Vajtai, Abhishek K. Singh, C. S. Tiwary, P. M. Ajayan, *Science Advances*, 4, e1701373 (2018)
14. A Non-van der Waals Two-Dimensional Material from Natural Titanium Mineral Ore Ilmenite, A. P. Balan, S. Radhakrishnan, R. Kumar, R. Neupane, S. K. Sinha, L. Deng, C. A. de los Reyes, A. Apte, B. M. Rao, M. Paulose, R. Vajtai, C. W. Chu, G. Costin, A. A. Martí, O. K. Varghese, Abhishek K. Singh, C. S. Tiwary, M. R. Anantharaman, and P. M. Ajayan, *Chem. Mater.*, 30, 5923 (2018)
15. An Insight into the Phase Transformation of WS_2 upon Fluorination, S. Radhakrishnan, D. Das, L. Deng, P. M. Sudeep, G. Colas, C. de los Reyes, S. Yazdi, C.-W. Chu, A. A. Martí, C. S. Tiwary, T. Filleter, Abhishek K. Singh, and P. M. Ajayan, *Adv. Mater.*, 1803366 (2018)

16. Elemental site occupancy in the $L1_2A_3B$ ordered intermetallic phase in Co-based superalloys and its influence on the microstructure, P. Pandey, S. K. Makineni, A. Samanta, A. Sharma, S. M. Das, B. Nithin, C. Srivastava, Abhishek K. Singh, D. Raabe, B. Gault, and K. Chattopadhyaya, *Acta Materialia*, 140, 163 (2018)
17. Morphology controlled synthesis of low bandgap $SnSe_2$ with high photodetectivity, R. K. Rai, S. Islam, A. Roy, G. Agrawal, Abhishek K. Singh, A. Ghosh and N. Ravishankar, Nanoscale 2018, In Press

3.13 Department of Physics (PHY)

3.13.1 Prof. Chandan Das Gupta's Lab

3.13.1.1Research

(a) Numerical studies of the role of vibrational modes in thermal transport in glass-forming liquids (b) Molecular dynamics studies of glassy systems of self-propelled particles with large persistence time at high density (c) Monte Carlo studies of phase transitions in multi-colour loop models.

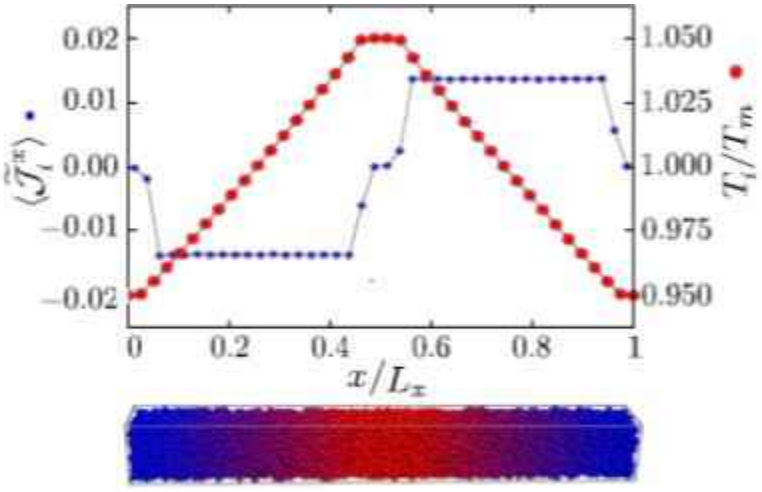

Fig. 1: Top panel: Local heat current density (left scale) and reduced temperature (right scale) along a rectangular sample (bottom panel) with the centre kept at a temperature higher than that at the ends.

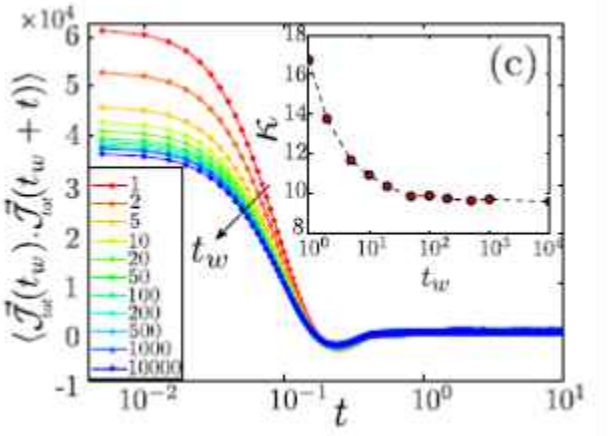

Fig. 2: Heat current time-correlation function with changing waiting time, plotted as a function of time. Inset: Dependence of the thermal conductivity on the waiting time.

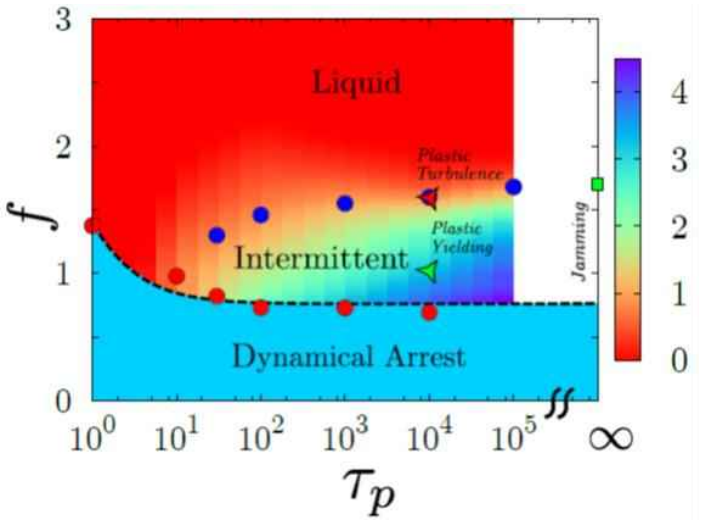

Fig.3: Phase diagram of a system of active particles in the activity (y axis) - persistence time (x axis) plane.

3.13.1.2 SERC Resources and Experiments

SahasraT, with number of cores varying from 200 to 12000. Tesla and the Fermi clusters with 4 GPU's where each GPU is made up of 240 processor cores.

8.59 million core hours of SahasraT were used.

3.13.1.3 Parallelization

The GPU programming was done using NVIDIA CUDA C libraries. The primary strategy employed was SIMD (single instruction multiple data), using a total of 512 block threads in lattice simulations. Home developed codes were parallelized for running on sahasraT using MPI (Message Passing Interface)

3.13.1.4 Performance

Depending upon the requirement, the execution time of our jobs on sahasraT ranged between 1 and 3 days. With the same core count, we have observed about 3 times speed-up in sahasraT compared to the cluster available in the Physics department.

3.13.1.5 Publications

1. S.K. Nandi, R. Mandal, P.J. Bhuyan, C. Dasgupta, M. Rao, and N.S. Gov (2018), A random first-order transition theory for an active glass, Proceedings of the National Academy of Sciences USA, vol. 115, 7688-7693.

2. R. Mandal, P. J. Bhuyan, P. Chaudhury, C. Dasgupta and M. Rao (2019), Extreme active matter at high densities, submitted to Nature Physics.

3. P. J. Bhuyan, R. Mandal, P. Chaudhury, A. Dhar and C. Dasgupta (2019), Aging effects on thermal conductivity of glass-forming liquids, submitted to Physical Review E.

3.13.2 Prof. H.R. Krishnamurthy's Lab

3.13.2.1 Research

Study of the novel properties in pyrochlores using first principles calculations

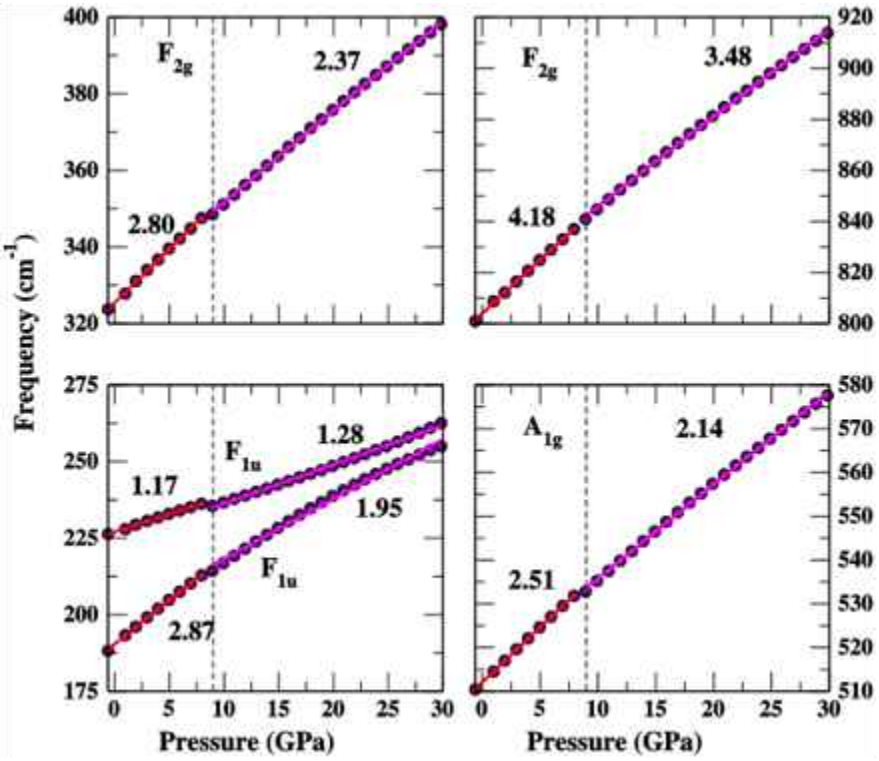

Fig. 1. Pressure dependent phonon frequencies of Dy2Ti2O7 pyrochlore showing structural phase transition around 9 Gpa pressure.

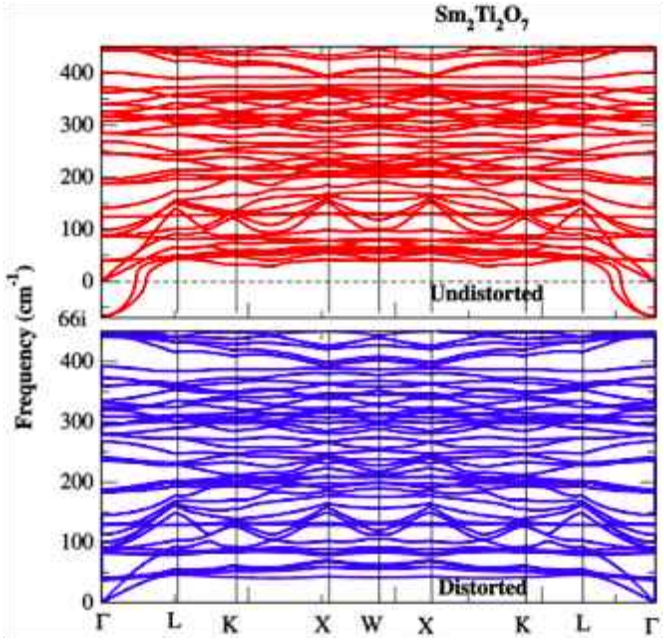

Fig. 2. Phonon band dispersion of Sm2Ti2O7 pyrochlore, showing the instability of the standard structure, and how a small distortion stabilizes the phonon spectra.

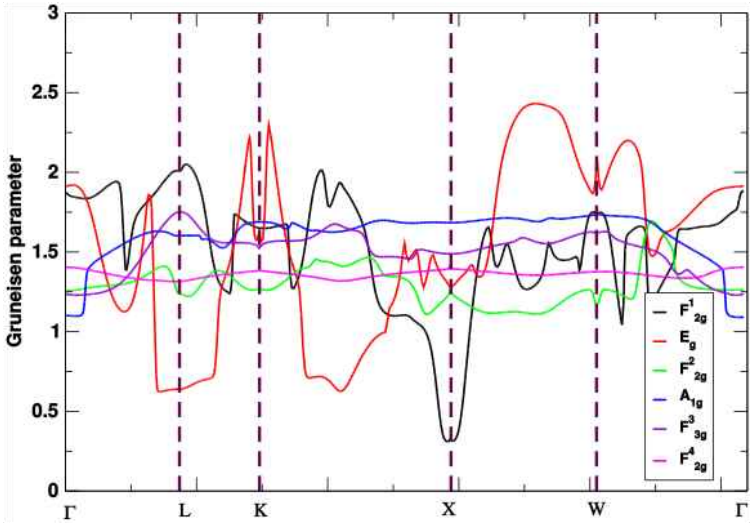

Fig. 3. Wave-vector dependence of the Gruneisen parameter of several phonon modes of Y2Ti2O7 pyrochlore shown along specific symmetry directions in the Brillouin zone. These form inputs to a ab-initio calculation of the thermal expansion of the material within the quasi-harmonic approximation.

3.13.2.2 SERC Resources and Experiments

Mostly we used the SahasraT supercomputer for all our calculations, and Delta cluster to some extent. We used around 800 cores for maximum allowed execution time queues of 24 hours and 72 hours, and we also used around 2000 cores for maximum allowed execution time queue of 24.

SahasraT Usage: 4.6 million core hours

3.13.2.3 Parallelization

We used quantum espresso code that is installed on SahasraT to perform all our calculations. The code is highly parallelized across the nodes.

3.13.2.4 Performance

SahasraT is much faster than any other systems available in our lab. Some of our works involved a heavy computational facility, which would not have been possible to carry out without SahasraT. At any given point of time we get minimum around 100 cores that is a great advantage.

3.13.2.5 Publications

1. Isostructural phase transition in Dy2ti2O7 pyrochlore (To be submitted)

2. A comparative study of the structural, elastic, thermal and vibrational properties in A2B2O7 (A=Sm, Gd, Tb, Dy, Ho, Er, Yb and Lu; B=Ti, Zr and Hf) pyrochlores (Manuscript under preparation)

Student: Soumen Kumar Bag

3.13.2.6 Research

Study of Correlation driven metallic and half-metallic phases in a band insulator

Fig.1 Phase diagram of t − t' Ionic Hubbard Model in t' -U plane at half-filling obtained using Dynamical mean Field Theory combined with Continuous Time Quantum Monte-Carlo impurity solver at βt =50.0, Δ = 1.0t. Here BI ≡ Band Insulator, PM ≡ Para magnetic Metal, FM ≡ Ferrimagnetic Metal, AFHM ≡ Anti-Ferromagnetic Half Metal, AFI ≡ Anti-Ferromagnetic Insulator. Across the line labelled UM the system goes from the BI to the PM state. Uc labels the phase transition line across which the system goes from a paramagnetic state to the magnetic state. UAFHM labels the line which separates the system's AFHM and FM phases. Finally, UAFI labels the line above which the system is an AFI.

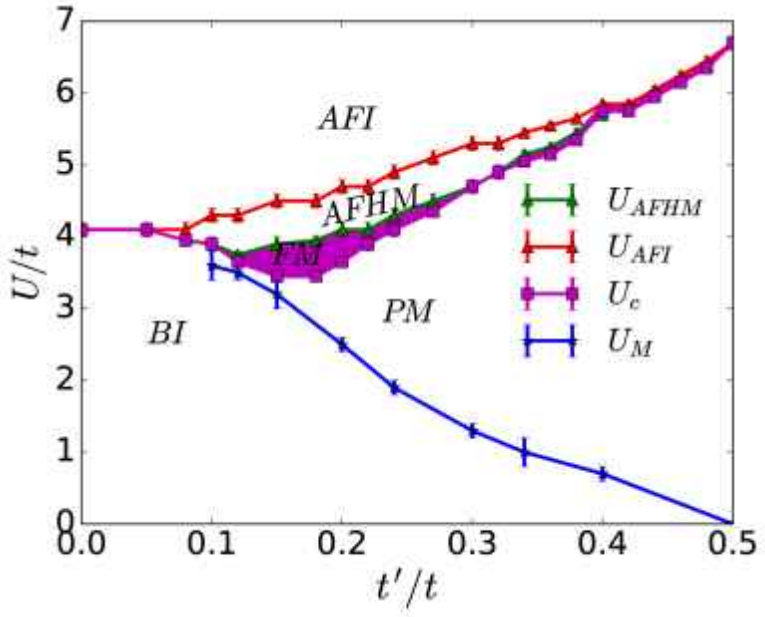

3.13.2.7 SERC Resources and Experiments

Mostly we used the SahasraT supercomputer for all our calculations. We used around 5 cores (120 Processor) for allowed execution time of 24 hours and 72 hours.

SahasraT Usage: 262254.21 CPU hours used

3.13.2.8 Publications

Correlation driven metallic and half-metallic phases in a band insulator (To be submitted)

3.13.3 Prof. Manish Jain's Lab

3.13.3.1Research

We studied the effect of twisting on the electronic and vibrational properties of bilayer transition metal dichalcogenides (TMDs) using density functional theory. Combining bilayers of two-dimensional materials with a small-angle twist between the layers leads to the formation of MoirÃ© superlattices with periodicity in the order of nanometers. Such superlattices can host a plethora of fascinating physics at the structural and electronic level. We explored twisted bilayer TMDs for such new and interesting physics.

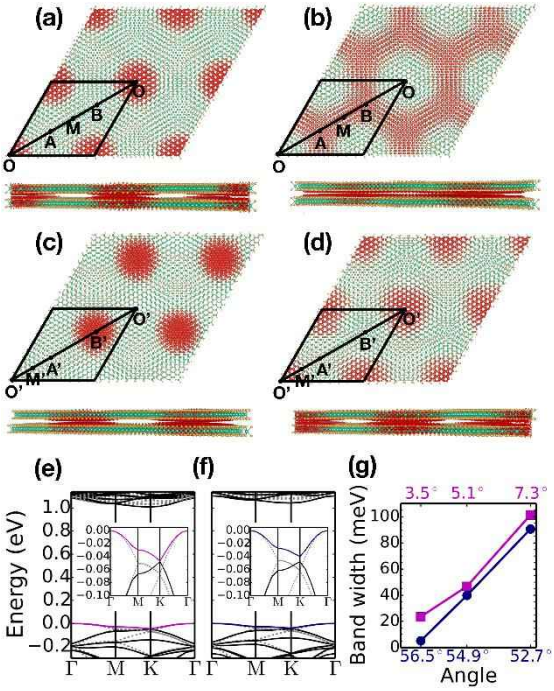

Charge density of the valence band maximum wave function in (a),(c) rigidly twisted [(b),(d) relaxed] 3.5° and 56.5° twisted MoS2 Moire superlattice, respectively. (e),(f) Band structure of the relaxed 5.1° and 54.9° twisted MoS2 Moire superlattice, respectively. The flatbands, near the valence band edge are shown with magenta and blue colors, respectively. The dashed line represents band structure of pure Bernal Mo on S and AB stacking for the same superlattice size, respectively. (Inset) An enlarged plot of the valence bands. (g) Variation of the bandwidth (in meV) with twist angle. The magenta line corresponds to angles approaching 0° and the blue line to angles approaching 60°.

3.13.3.2 SERC Resources and Experiments

We used > 10,000 CPU cores on Sahasrat for some of the runs.

SahasraT usage: 13.62 million CPU core hours.

3.13.3.3 Parallelization

Hybrid parallelization -- both openMP and MPI. Quantum Espresso uses parallel FFTs, parallelization of dense matrix vector products and iterative diagonalization techniques.

3.13.3.4 Performance

Several runs required multiple large queue jobs on Sahasrat. This would not be possible on any local machine that we/department owns.

3.13.3.5 Publications

[1] Mit H. Naik and Manish Jain, Physical Review Letters, 121, 266401 (2018).

[2] Mit H. Naik and Manish Jain, Physical Review Materials, 2, 084002 (2018).

[3] Indrajit Maity, Prabal K. Maiti, and Manish Jain, Physical Review B, 97, 161406(R) (2018).

[4] Mit H. Naik and Manish Jain, Computer Physics Communications, 226, 114 (2018).

[5] Sudipta Kundu, Satadeep Bhattacharjee, Seung-Cheol Lee, and Manish Jain, Computer Physics Communications, 233, 261 (2018).

[6] Sahil Tippireddy, Raju Chetty, Krushna Kumari Raut, Mit H. Naik, Prashanta K. Mukharjee, Manish Jain, R. Nath, Krzysztof Wojciechowski, and Ramesh Chandra Mallik, Physical Chemistry Chemical Physics, 20, 28667 (2018).

[7] Sahil Tippireddy, Raju Chetty, Mit H. Naik, Manish Jain, Kamanio Chattopadhyay, and Ramesh Chandra Mallik, The Journal of Physical Chemistry C, 122, 8735 (2018).

[8] K. S. Vasu, Debabrata Pramanik, Sudipta Kundu, Sridevi S., N. Jayaraman, Manish Jain, Prabal K. Maiti, and A. K. Sood, Journal of Materials Chemistry C, 6, 6483 (2018).

3.13.4 Prof. Prabal Maiti's Lab

SahasraT usage: 13.54 million CPU core hours.

Student: ANIL KUMAR SAHOO

3.13.4.1Research

Force probe methods are routinely used to study conformational transitions of biomolecules at single-molecule level. In contrast to simple kinetics, some proteins show complex response to mechanical perturbations that is manifested in terms of unusual force-dependent kinetics. Here, we study, via fully atomistic molecular dynamics (MD) simulations, constant force-induced unfolding of ubiquitin protein. Our simulations reveal a crossover at an intermediate force (about 400 pN) in the unfolding rate versus force curve. We find by calculation of multidimensional free energy landscape (FEL) of the protein that the complex unfolding kinetics is intimately related to the force dependent modifications in the FEL. The crossover in the rate can be explained in terms of an interplay between entropy and enthalpy with relative importance changing from low force to high force. We rationalize the results by using multidimensional transition state theory.

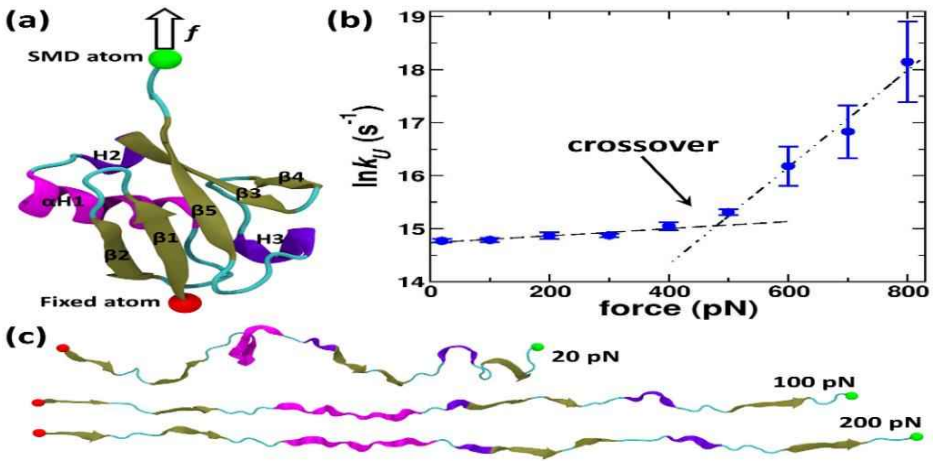

Figure 1: Unfolding simulation protocol and the force dependent unfolding rates. (a) The native structure of protein ubiquitin is depicted in the secondary structure (SS) representation, where its SSs are named. The N-terminal Cα atom (red sphere) is fixed, and a constant force, f, is applied to the C-terminal Cα atom (green sphere) to unfold the protein completely. (b) Natural logarithm of the unfolding rate, kU, as a function of the pulling force is shown. (c) The unfolded structures of the protein for different forces are shown.

3.13.4.2 SERC Resources and Experiments

Good scalability up to 44 nodes per job for running Molecular Dynamics simulations using NAMD package.

3.13.4.3 Parallelization

Message Passing Interface (MPI).

3.13.4.4 Performance

Two times faster in case of SERC compared to lab system (used packages: AMBER, NAMD).

3.13.4.5 Publications

Anil Kumar Sahoo, Biman Bagchi and Prabal K. Maiti, Unfolding Dynamics of Ubiquitin from Constant Force MD Simulation: Entropy-Enthalpy Interplay Shapes the Free Energy Landscape, J. Phys. Chem. B, 2019 (just accepted manuscript).

Student: **BISWAJIT GORAI**

3.13.4.6 Research

The glycoprotein 41 (gp41) of HIV helps to mediate the fusion of viral and host membranes. The detailed mechanism of host cell invasion remains obscure due to the unavailability of experimental structure of complete gp41. In the current study the post-fusion (PoF) trimeric structure of ecto-domain including transmembrane domain of gp41 was modeled using multiple homologous templates of SIV and HIV-1. The HIV-1 gp41 structure developed in this work can be used in future studies to gain insight into the mechanism of virus invasion and probing potent inhibitor to eliminate AIDS.

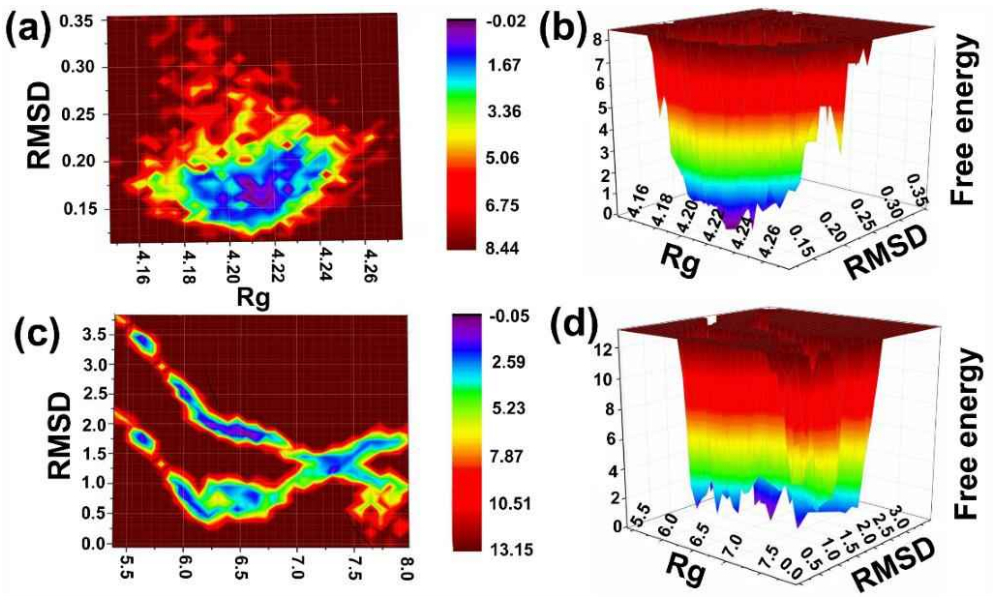

Figure 2. Contour plots representing the free-energy landscape (FEL) of post-fusion (PoF) conformer ('a' – 2D and 'b' – 3D) and pre-fusion (PrF) conformer ('c' – 2D and 'd' – 3D) of HIV gp41 is shown here. RMSD and Rg are selected as reaction coordinates to obtain the relative Gibbs free energy change (kJ/mol).

3.13.4.7 SERC Resources and Experiments

20 to 60 nodes per job (depending on the size of the system).

3.13.4.8 Parallelization

Message Passing Interface (MPI)

3.13.4.9 Performance

Around two times faster in case of SERC compared to lab system (used GROMACS simulation tool)

3.13.4.10 Publications

B. Gorai, S. Das and P. K. Maiti, Prediction and validation of HIV-1 gp41 ecto-transmembrane domain post-fusion trimeric structure using molecular modelling, (Submitted).

Student: **IPSITA BASU**

3.13.4.11 Research

SiRNA is known to be responsible for specific gene silencing mechanism. For in vivo application of SiRNA, the intracellular entry is required via crossing the membrane barrier which is the primary challenge as it is negatively charged molecules and thus can't enter cells by themselves. In this problem, we have attempted a range of approaches with different carriers to find out the most efficient carrier for SiRNA intracellular delivery.

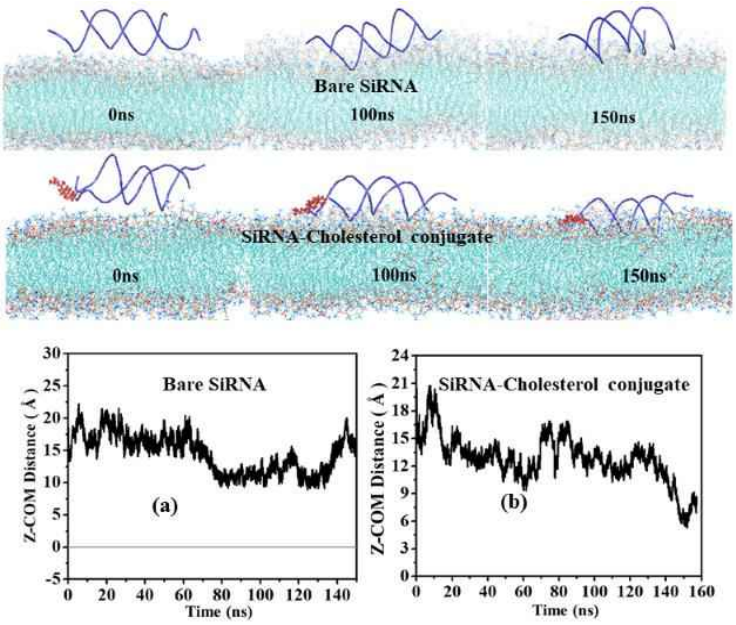

Figure 3: (Top Panel) Time dependent snapshots of the Bare SiRNA and SiRNA-Cholesterol conjugate in DMPC lipid bilayer. (Bottom Panel) Z-Distance between the center of mass of Bare SiRNA and SiRNA-Cholesterol conjugate complex and that of the phosphate group of the respective monolayer of DMPC bilayer with time.

3.13.4.12 SERC Resources and Experiments

20-50 nodes per job.

3.13.4.13 Parallelization

Message Passing Interface (MPI)

3.13.4.14 Performance

Faster compared to lab system in AMBER simulation.

Student: **MOUNIKA GOSIKA**

3.13.4.15 Research

Understanding dendrimer - cell membrane interactions are crucial for investigating the drug-delivery, gene therapy applications of the dendrimers. We have employed fully atomistic molecular dynamics simulations to probe these interactions using three widely used force fields namely GAFF, CHARMM and GROMOS. Surprisingly, the interaction seems to be dependent on the FF, we tried to explain this discrepancy from the dendrimer's hydration, van der Waals and electrostatic energies of the interaction. We have now extended this problem to understand the dendrimer - model cell membrane's interaction via surface potentials of the dendrimer, membrane.

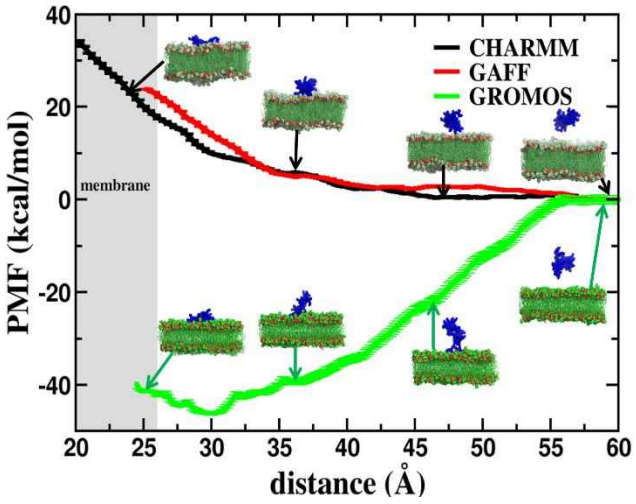

Figure 4: The potential of mean force calculations as a function of the dendrimer centre of mass(com) to lipid com z-distance. In case of GROMOS, there is attractive interaction, but the interactions are repulsive in nature for GAFF and CHARMM cases.

3.13.4.16 SERC Resources and Experiments

SERC's Cray machine is used for all the simulations. 10-20 nodes are used for the CPU jobs (GROMOS, NAMD packages). For AMBER18 GPU runs 2-4 GPU nodes are used.

3.13.4.17 Parallelization

Message Passing Interface (MPI)

3.13.4.18 Performance

AMBER – 10 ns/day (0.3 million atoms) (20 CPU nodes/ 2 GPU nodes), GROMACS – 66 ns/day (5 CPU nodes) (0.1 million atoms), and NAMD – 12 ns/day (0.1 million atoms) (44 CPU nodes).

3.13.4.19 Publications

1. S. Kanchi, M. Gosika, K. G. Ayappa, P. K. Maiti, Dendrimer Interactions with Lipid Bilayer: Comparison of Force Field and Effect of Implicit vs Explicit Solvation, J. Chem. Theory Comput., 2018, 14 (7), pp 3825–3839.

2. M. Gosika, S. Kanchi and P. K. Maiti, Revisiting the Interaction of Nanoparticles with Lipid Bilayers: Role of Electrostatics Description in MD Simulations (In preparation).

Student: **SUPRIYO NASKAR**

3.13.4.20 Research

6-helix DNA nanotubes (DNTs) are the recent addition to the growing repository of the DNA based nanostructures and receiving attention because of their application as robotic arm in drug delivery and in designing synthetic membrane spanning nanopores. The structural stability and rigidity are the most important measurements of these novel nanostructures. In this article, we took one step further and proposed an efficient method for increasing the stability of DNTs. Using several hundred long all atom molecular dynamics (MD) simulation we have attempted to understand and explain the effects of increasing the salt concentration on the structural stability of the DNTs. We thoroughly examined the structural properties of the DNA nanotubes in different physiological condition. Starting with monovalent ion NaCl and KCl, we

also explained the effect of divalent cation (Mg2+) concentration on DNT rigidity. Using measures like contour length distribution, bending angle distribution we quantify their elastic properties like stretch modulus, persistence length which has been verified experimentally. Remarkably, we find our results consistent compared to those proposed by experiments.

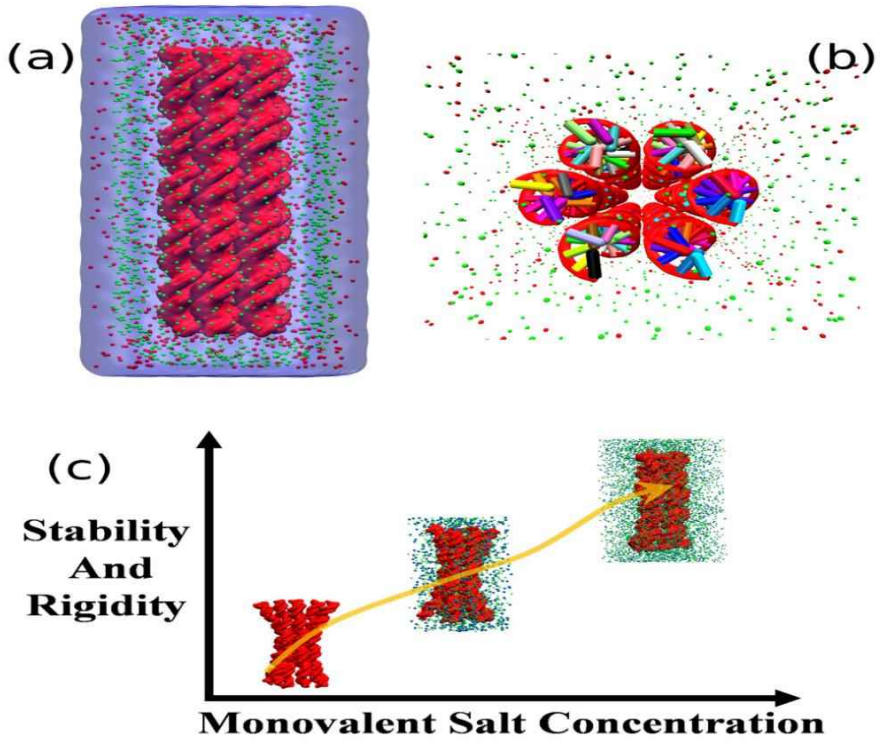

Figure 6. (a) Initially built DNT immersed in a rectangular water box with Na+ ions and excess salt (NaCl). The green and red dots represent the Na+ and Cl- ions respectively. (b) Top View of the same system without any explicit water. (c) Key finding of the study using a graphical representation.

3.13.4.21 SERC Resources and Experiments

SERC's cray machine is used for all the simulations. 2-4 GPU nodes are used for the AMBER18 GPU runs. For visualization of the atomistic structure we used cray dell visualization servers.

3.13.4.22 Parallelization

GPU (CUDA) Version of PMEMD.

3.13.4.23 Performance

10 ns/day (0.3 million atoms) (2 to 4 GPU nodes).

3.13.4.24 Publications

Supriyo Naskar, Mounika Gosika, Himanshu Joshi and Prabal K. Maiti, Tuning the Stability of DNA Nanotubes with Salt, Journal of Physical Chemistry C (Under Review).

3.13.5 Prof. Rahul Pandit's Lab

Team: Mr Akhilesh Kumar Verma, Prof. Rahul Pandit

3.13.5.1 Research

We are trying to calculate velocity structure functions for superfluid turbulence at the level of the HVBK model. High-order structure function help us to study deviations from the Gaussian behaviour. In the recent past, many experiment have been done to study the structure function exponents in superfluid turbulence, we are carrying out the most detailed study of such exponents by using direct numerical (pseudospectral) simulations.

3.13.5.2 SERC Resources and Experiments

We have used 512 cores of Cray XC 40.

SahasraT usage: 2.04 million CPU core hours.

3.13.5.3 Parallelization

We have used MPI parallelization. We are studying the 3D problem and we have done parallelization along the Z axis.

3.13.5.4 Performance

Our runs take nearly 36 hours on the Cray.

Team: Ms KV Sai Swetha, Mr Puneet Sharma and Prof. Rahul Pandit

3.13.5.5Research

Numerical studies of the 3D Euler equation and 3D hyperviscous Navier-Stokes equations

We solve the three-dimensional Euler equation in a cylindrical geometry by using a pseudospecttral Fourier-Chebyshev code that we have developed. The main purpose is to see if the solution of this Euler equation develop a finite-time singularity for a certain initial and the above boundary conditions.

- Studies on the development of a potential singularity in the 3D axisymmetric Euler equations using a Fourier-Chebyshev pseudospectral method on 2D meshes. Aiming for achieveing resolutions upto 2048. Libraries used are LAPACK, BLAS and FFTW-3. Systems used: SahasraT CRAY, Dell-Vis1.
- Studies on the mixing of passive scalars by ann underlying turbulent flow, including cases where the dissipation in the turbulent velocity field is due to hyperviscosity. Determining and quantifying any effecs of the bottleneck developed in the velocity spectra on the spectra of the advected scalars

Packages used: FFTW, BLAS, LAPACK

3.13.5.6SERC Resources and Experiments

Cores used ~256 per run, execution time ~1-day per run. No.of jobs:143 Core hours used: 100228

4. Grand Challenge Executions on SahasraT

SERC conducted a Grand Challenge demonstration contest on October 30 2018, where it encouraged the Institute users to utilize almost the full capacity of SahasraT for executions of a single application, i.e., a parallel job spanning the entire machine!

SERC received three entries, from physics, aerospace and materials, respectively, where each of them was given 8 hours to perform runs at full and half scale. All these three runs completed successfully,

utilizing more than 31,000 CPU cores! These are the largest runs ever executed on SahasraT, and hence the Institute, and perhaps the largest runs for such varied applications carried out in the country too!

Following are the details of these three applications

4.1 Mass accretion into Black Holes

Team: Prasun Dhang, Prof. Prateek Sharma, Department of Physics

Report:
https://indianinstituteofscience-my.sharepoint.com/:b:/g/personal/vss_iisc_ac_in/EZLRKv600M5JkyoWWa6meQUBrLeYIxY6tUGKBMKXbZ8J4g?e=2i5sDz

4.2 Numerical Simulation of Shock Turbulence Interactions

Team: Sumit Patel, Prof. Joseph Matthew, Aerospace Engineering

Report:

https://indianinstituteofscience-my.sharepoint.com/:b:/g/personal/vss_iisc_ac_in/EdYIDSw4Vb9FkSZtcya46oYBMlIfL5SoA4SsA2pbDq7pmg?e=IeGb40

4.3 Microstructure Evolution in Multi-phase Eutectic Alloys

Team: Sumeet Khanna, Prof. Abhik Choudhury

Report:

https://indianinstituteofscience-my.sharepoint.com/:b:/g/personal/vss_iisc_ac_in/EXiXtf2N8nJClEpv8n-ZwysBs0ErzEEmMHcHbBZcPLeUVg?e=YfLWIc

5. Publications in 2018 using SahasraT

1. Praveen Kumar B., N. Balakrishnan, Prediction of Longitudinal Dynamic Derivatives for TransCruiser Aircraft from Unsteady RANS Computations, Symposium on Applied Aerodynamics and Design of Aerospace Vehicles, 28 November – 1 December, 2018, Royal Orchid Resort & Convention Center, Bangalore, India.
2. Navneet A Gopinath, Munikrishna N, Nikhil V Shende, N. Balakrishnan, High lift JAXA Standard Model (JSM) flow prediction using CFD solver HiFUN, Symposium on Applied Aerodynamics and Design of Aerospace Vehicles, 28 November – 1 December, 2018, Royal Orchid Resort & Convention Center, Bangalore, India.
3. Mohamed Yousuf, N. Balakrishnan, Residual based mesh adaptation for Meshless LSFD-U solver, AIAA Journal, https://doi.org/10.2514/1.J057633.

4. Rintu Panja, Sathish Vadhiyar. A Multi-Node Multi-Device Parallel Boruvka's MST Algorithm. In the proceedings of the *International Conference on Parallel Processing (ICPP)*, August 2018, Eugene, USA.
5. Arnab Kabiraj and Santanu Mahapatra, "High-throughput first-principles-calculations based estimation of lithium ion storage in monolayer rhenium disulfide" Communications Chemistry, Nature Publishing Group (NPG), 2018.
6. Jyothish Joy, Eluvathingal D. Jemmis, Contrasting Behavior of the Z-Bonds in X-Z···Y Weak Interactions: Z = Main Group Elements Versus the Transition Metals, Inorg. Chem. 56, 1132-1143 (2017).
7. Jyothish Joy, Eluvathingal D. Jemmis, A Halogen Bond Route to Shorten the Ultrashort Sextuple Bond in Cr_2 and Mo_2, Chem. Commun. 53, 8168-8171 (2017).
8. Joy Jyothish, E. Akhil and E. D. Jemmis, Halogen bond shortens and strengthens the bridge bond of [1.1.1]propellane and the open form of [2.2.2]propellane. Phys. Chem. Chem. Phys., DOI: 10.1039/c8cp05125a (2018).
9. Naiwrit Karmodak, Eluvathingal D. Jemmis, Role of Holes in borophenes: an ab-initio study of the structure and stability with and without metal template, Angew. Chem. 56, 10093-10097 (2017).
10. Naiwrit Karmodak, E. D. Jemmis, Metal Templates and Boron Sources Controlling Borophene Structures: An Ab Initio Study, J. Phys. Chem. C, 122, 2268-2274 (2018).
11. Naiwrit Karmodak, Eluvathingal D. Jemmis, Dynamic behavior of the exohedral transition metal complexes of B_{40}: eta6- and eta7-$B_{40}Cr(CO)_3$ and $Cr(CO)_3$-eta7-B_{40}-eta7-$Cr(CO)_3$, J. Chem. Sci. 129, 1061-1067 (2017).
12. Naiwrit Karmodak, Eluvathingal D. Jemmis, Fragment approach to the electronic structure of tau-boron allotrope, Phys. Rev. B, 95, 165128 (2017).
13. Sagar Ghorai, Eluvathingal D. Jemmis, A DFT study of the stabilization of B-B triple bond in a metallaborocycle: Contrasting electronic structures of boron and carbon analogs, Chem. Eur. J. 23, 9746-9751 (2017).
14. Sagar Ghorai, E. D. Jemmis, B-B coupling and B-B catenation: Computational study of the structure and reactions of metal-bis(borylene) complexes. Chem. Eur. J., DOI: 10.1002/chem.201804599 (2018).
15. S. Marutheeswaran and E. D. Jemmis, Adamantane-Derived Carbon Nanothreads: High Structural Stability and Mechanical Strength, J. Phys. Chem. C, 2018, 122 (14), pp 7945-7950.
16. Sourav Ghosh, Punarbasu Roy, Naiwrit Karmodak, E. D. Jemmis, Govindasamy Mugesh, Nanoisozymes: Crystal Facet-Dependent Enzyme Mimetic Activity of V2O5 Nanomaterials, Angew. Chem. Int.Ed. 130, 4600-4605 (2018).
17. A. Ramaraj, K. Hari Krishna Reddy, Helena Keil, Dietmar Stalke, Eluvathingal D. Jemmis, and Balaji R. Jagirdar, Approaches to Sigma-complexes via Displacement of Agostic Interactions: an Experimental and Theoretical Investigation, Organometallics, 36, 2736-2745 (2017). Shyama Ramakrishnan, E. D. Jemmis, Origin of beta-agostic interaction in d0-transition metal alkyl complexes: Influence of ligands, J. Organomet. Chem., 865, 37-44 (2018).
18. Ramkumar Kannan, Sandeep Kumar, Alex Andrews, Eluvathingal D. Jemmis, and Ajay Venugopal, Consequence of Ligand Bite Angle on Bismuth Lewis Acidity, Inorg. Chem. 56, 9391-9395 (2017).
19. Bijan Mondal, Ranjit Bag, Sagar Ghorai, K Bakthavachalam, E. D. Jemmis, Sundargopal Ghosh, Synthesis, Structure, Bonding and Reactivity of Metal Complexes comprising Diborane(4) and Diborene(2): [{Cp*Mo(CO)2}2{μ-?n2:n2-B2H4}] and [{Cp*M(CO)2}2B2H2M(CO)4], M=Mo,W. Angew. Chem. Int.Ed. , 57, 8079-8083 (2018).

20. B. Bhadak, R. Sankarasubramanian, A. Choudhury, Metall and Mat Trans A (2018), 49:57055726., Phase eld modeling of equilibrium shapes of the precipitate under infuence of the coherency stresses.
21. S. Khanna, A.S. Kiran, A. Choudhury, Seventh International Conference on Solidi cation Science and Processing (ICSSP-2018).
22. F. Kaka, P.C. Ramamurthy, A. Choudhury, International Conference on Emerging Electronics (ICEE), IEEE-2018.
23. Kumar Gayatri, Richa Mudgal, Narayanaswamy Srinivasan, and Sankaran Sandhya. "Use of designed sequences in protein structure recognition." Biology direct 13, no. 1 (2018): 8.
24. Journal Proteins:SFB (Ghosh, S., Gadiyaram, V., and Vishveshwara, S.(2017). Validation of Protein Structure Models using Network Similarity Score. Proteins: Structure, Function and Bioinformatics, 85(9) 1759-1776)
25. High Thermoelectric Figure of Merit via Tunable Valley Convergence Coupled Low Thermal Conductivity in $A^{II}B^{IV}C^{V}_2$ Chalcopyrites, M. Mukherjee, G. Yumnam, and Abhishek K. Singh, *J. Phys. Chem. C* 122, 51, 29150 (2018)
26. Amine Functionalized Zirconium Metal-Organic Framework as an Effective Chemiresistive Sensor for Acidic Gases, M. E. DMello, N. Sundaram, A. Singh, Abhishek K. Singh and S. B. Kalidindi, *Chem. Commun.*, 2019,55, 349-352
27. Engineering Defect Transition-Levels through van der Waals Heterostructure, A. Singh, A. Manjanath and Abhishek K. Singh, *J. Phys. Chem. C* 122, 24475 (2018)
28. Synergistic Core-shell Interactions Enable Ultra-low Overpotentials for Enhanced CO_2 Electro-reduction Activity, R. Ahmad and Abhishek K. Singh, *J. Mater. Chem. A* 6, 21120 (2018)
29. Multiple Triple-Point Fermions in Heusler Compounds, R. K. Barik, R. L. Shinde, and Abhishek K. Singh, *J. Phys. Cond. Mat.* 30, 375702 (2018)
30. Nonlinear Polarization and Low-Dissipation Ultrafast Optical Switching in Phosphorene, R. Shinde, and Abhishek K. Singh, *J. Phys. Chem. C* 122, 19146 (2018)
31. Machine-Learning-Assisted Accurate Band Gap Predictions of Functionalized MXene, A. C. Rajan, A. Mishra, S. Satsangi, R. Vaish, H. Mizuseki, K. R. Lee and Abhishek K. Singh, *Chem. Mater.* 30, 4031 (2018)
32. Pressure-Induced Topological Phase Transitions in $CdGeSb_2$ and $CdSnSb_2$, R. Juneja, R. Shinde, and Abhishek K. Singh, *J. Phys. Chem. Lett.* 9, 2202 (2018)
33. Structural, Vibrational, and Electronic Topological Transitions of $Bi_{1.5}Sb_{0.5}Te_{1.8}Se_{1.2}$ under Pressure, J. S. Kim, R. Juneja, N. P. Salke, W. Palosz, V. Swaminathan, S. Trivedi, and Abhishek K. Singh, D. Akinwande and J. Lin, *J. Appl. Phys*. 123, 115903 (2018)
34. Interplay of Structural and Bonding Characters in Thermal Conductivity and Born-Effective Charge of Transition Metal Di chalcogenides, G. Yamnam, T. Pandey, and Abhishek K. Singh, *J. Phys. Chem. C* 122, 2521 (2018)
35. C_2N/WS_2 Van der Waals Type-II Heterostructure as a Promising Water Splitting Photocatalyst, R. Kumar, D. Das, and Abhishek K. Singh, *J. Catal.* 359, 143 (2018)
36. Origami inspired Three-Dimensional Interconnected Molybdenum Carbide Nanoflakes, R. Koizumi, S. Ozden, A. Samanta, A. P. Alves, A. Mishra, G. Ye, G. G. Silva, R. Vajtai, Abhishek K. Singh, C. S. Tiwary, and P. M. Ajayan, *Adv. Mater. Interfaces*, 1701113 (2018)
37. Atomically thin gallium layers from solid-melt exfoliation, V. Kochat*, A. Samanta*, Y. Zhang, S. Bhowmick, P. Manimunda, S. A. S. Asif, A. Stender, R. Vajtai, Abhishek K. Singh, C. S. Tiwary, P. M. Ajayan, *Science Advances*, 4, e1701373 (2018)
38. A Non-van der Waals Two-Dimensional Material from Natural Titanium Mineral Ore Ilmenite, A. P. Balan, S. Radhakrishnan, R. Kumar, R. Neupane, S. K. Sinha, L. Deng, C. A. de los Reyes,

A. Apte, B. M. Rao, M. Paulose, R. Vajtai, C. W. Chu, G. Costin, A. A. Martí, O. K. Varghese, Abhishek K. Singh, C. S. Tiwary, M. R. Anantharaman, and P. M. Ajayan, *Chem. Mater.*, 30, 5923 (2018)

39. An Insight into the Phase Transformation of WS_2 upon Fluorination, S. Radhakrishnan, D. Das, L. Deng, P. M. Sudeep, G. Colas, C. de los Reyes, S. Yazdi, C.-W. Chu, A. A. Martí, C. S. Tiwary, T. Filleter, Abhishek K. Singh, and P. M. Ajayan, *Adv. Mater.*, 1803366 (2018)
40. Elemental site occupancy in the $L1_2A_3B$ ordered intermetallic phase in Co-based superalloys and its influence on the microstructure, P. Pandey, S. K. Makineni, A. Samanta, A. Sharma, S. M. Das, B. Nithin, C. Srivastava, Abhishek K. Singh, D. Raabe, B. Gault, and K. Chattopadhyaya, *Acta Materialia*, 140, 163 (2018)
41. Morphology controlled synthesis of low bandgap $SnSe_2$ with high photodetectivity, R. K. Rai, S. Islam, A. Roy, G. Agrawal, Abhishek K. Singh, A. Ghosh and N. Ravishankar, Nanoscale 2018, In Press
42. S.K. Nandi, R. Mandal, P.J. Bhuyan, C. Dasgupta, M. Rao, and N.S. Gov (2018), A random first-order transition theory for an active glass, Proceedings of the National Academy of Sciences USA, vol. 115, 7688-7693.
43. R. Mandal, P. J. Bhuyan, P. Chaudhury, C. Dasgupta and M. Rao (2019), Extreme active matter at high densities, submitted to Nature Physics.
44. P. J. Bhuyan, R. Mandal, P. Chaudhury, A. Dhar and C. Dasgupta (2019), Aging effects on thermal conductivity of glass-forming liquids, submitted to Physical Review E.
45. Mit H. Naik and Manish Jain, Physical Review Letters, 121, 266401 (2018).
46. Mit H. Naik and Manish Jain, Physical Review Materials, 2, 084002 (2018).
47. Indrajit Maity, Prabal K. Maiti, and Manish Jain, Physical Review B, 97, 161406(R) (2018).
48. Mit H. Naik and Manish Jain, Computer Physics Communications, 226, 114 (2018).
49. Sudipta Kundu, Satadeep Bhattacharjee, Seung-Cheol Lee, and Manish Jain, Computer Physics Communications, 233, 261 (2018).
50. Sahil Tippireddy, Raju Chetty, Krushna Kumari Raut, Mit H. Naik, Prashanta K. Mukharjee, Manish Jain, R. Nath, Krzysztof Wojciechowski, and Ramesh Chandra Mallik, Physical Chemistry Chemical Physics, 20, 28667 (2018).
51. Sahil Tippireddy, Raju Chetty, Mit H. Naik, Manish Jain, Kamanio Chattopadhyay, and Ramesh Chandra Mallik, The Journal of Physical Chemistry C, 122, 8735 (2018).
52. [8] K. S. Vasu, Debabrata Pramanik, Sudipta Kundu, Sridevi S., N. Jayaraman, Manish Jain, Prabal K. Maiti, and A. K. Sood, Journal of Materials Chemistry C, 6, 6483 (2018).
53. Anil Kumar Sahoo, Biman Bagchi and Prabal K. Maiti, Unfolding Dynamics of Ubiquitin from Constant Force MD Simulation: Entropy-Enthalpy Interplay Shapes the Free Energy Landscape, J. Phys. Chem. B, 2019 (just accepted manuscript).
54. 1. S. Kanchi, M. Gosika, K. G. Ayappa, P. K. Maiti, Dendrimer Interactions with Lipid Bilayer: Comparison of Force Field and Effect of Implicit vs Explicit Solvation, J. Chem. Theory Comput., 2018, 14 (7), pp 3825–3839.
55. Thejna, T., G. Bala, N.Devaraju and R. Nemani, 2018: Potential roles of CO_2 fertilization, climate warming, nitrogen deposition and land use and land cover change on the global terrestrial carbon uptake in the 21st century, Climate Dynamics, https://doi.org/10.1007/s00382-018-4388-8
56. Muthyala, R., G. Bala, and A. Nalam, 2018: Regional scale analysis of climate extremes in an SRM geoengineering simulation, Part 1: Precipitation Extremes, Current Science, 114 (5), 1024-1035
57. Muthyala, R., G. Bala, A. Nalam, 2018: Regional scale analysis of climate extremes in an SRM geoengineering simulation, Part 2: Temperature Extremes, Current Science, 114 (5), 1036-1045
58. Modak, A., G. Bala, K. Caldeira, and L. Cao, 2018: Does shortwave absorption by Methane

influence its effectiveness? Climate Dynamics, https://doi.org/10.1007/s00382-018-4102-x

59. Sahil Tippireddy, Raju Chetty, Mit H. Naik, Manish Jain, Kamanio Chattopadhyay, Ramesh Chandra Mallik, "Electronic and thermoelectric properties of transition metal substituted tetrahedrite", *J. Phys. Chem. C*, 122, 8735 (2018).
60. Sahil Tippireddy, Raju Chetty, Krushna Kumari Raut, Prashanta K. Mukherjee, Mit H. Naik, R. Nath, Manish Jain, Krzysztof Wojciechowski, Ramesh Chandra Mallik, "Electronic and thermoelectric properties of Zn and Se double substituted tetrahedrite", *Phys. Chem. Chem. Phys.* 20, 28667 (2018).
61. Prem Kumar D. S, Sahil Tippireddy, Anbalagan Ramakrishnan, Kuei-Hsien Chen, P. Malar, Ramesh Chandra Mallik, "Thermoelectric and electronic properties of Chromium substituted tetrahedrite", *Semicond. Sci. Technol.* 34, 035017 (2018).
62. Dendrimer: A Novel Nanomaterial, Debabrata Pramanik, Subbarao Kanchi, K. G. Ayappa and Prabal K. Maiti, *Springer Series in Materials Science Computational Materials, Chemistry, and Biochemistry: From Bold Initiatives to the Last Mile.* In Press (2018).
63. Influence of Surface Commensurability on the Structure and Relaxation Dynamics of a Confined Monatomic Fluid, V. Vadhana, Chandan Dasgupta and K. G. Ayappa, *Journal of Chemical Physics*, 149, 064503 (2018).
64. Dendrimer Interactions with Lipid Bilayer: Comparison of Force Field and Effect of Implicit vs Explicit Solvation, Subbarao Kanchi, Mounika Gosika, K. G. Ayappa and Prabal K. Maiti, *J. Chem. Theory Comput.*, 14, 3825–3839 (2018).
65. Cholesterol Promotes Cytolysin A Activity by Stabilizing the Intermediates During Pore Formation, Pradeep Sathyanarayana, Satyaghosh Maurya, Amit Behera, Monisha Ravichandran, Sandhya S. Visweswariah, K. Ganapathy Ayappa, Rahul Roy, *Proceedings of the National Academy of Sciences* 115, E7323-E7330 (2018)
66. D. Prasad, P. Sharma, A. Babul, "Cool-Core Clusters : Role of BCG, Star Formation, and AGN-Driven Turbulence," Astrophysical Journal, 863, 62 (2018)
67. S. Gupta, B. B. Nath, P. Sharma, "Constraining cosmic ray acceleration in young star clusters using multi-wavelength observations," Monthly Notices of Royal Astronomical Society, 479, 5220 (2018)
68. A. Vijayan, K. C. Sarkar, B. B. Nath, P. Sharma, Y. Shchekinov, "Extra-planar X-ray emission from disc-wide outflows in spiral galaxies," Monthly Notices of Royal Astronomical Society, 475, 5513 (2018)
69. R. K. Reddy A and S. N. Punnathanam, "Calculation of excess free energy of molecular solids comprised of flexible molecules using Einstein molecule method", Mol. Sim., DOI: 10.1080/08927022.2018.1450984 (2018)
70. H. Maity, A.N. Muttathukattil and G. Reddy*, "Salt effects on protein folding thermodynamics",*J. Phys. Chem. Lett.*,9, 5063, 2018.
71. H. Maity and G. Reddy*, "Transient intermediates are populated in the folding pathways of single domain two state folding Protein L", *J. Chem. Phys.*, 148, 165101, 2018.
72. H. Maity and G. Reddy*, "Thermodynamics and kinetics of single chain Monellin folding with structural insights into specific collapse in the denatured state ensemble", *J. Mol. Biol.*,430, 465, 2018.
73. B. Biswas, A.N. Muttathukattil, G. Reddy*, and P. Singh*,"Contrasting effects of guanidinium chloride and urea on the activity and unfolding of Lysozyme", *ACS Omega., 3, 14119,* 2018.

6. Projects Based on SahasraT

1. Reversing Climate Change Via Geoengineering: Impacts on developing countries like India" Prof. G Bala, CAOS. DST, Major R&D Program grant for April 2017-April 2020

2. Understanding the interactions of pore forming toxins: Influence of cholesterol, membrane computation and asymmetry. Prof. Ganapathy Ayyappa. DST. Ongoing.
3. Bacterial membrance modelling and interaction with small molecules. Prof. Ganapathy Ayyappa. DST. Ongoing.
4. Low-energy purification of drinking water by engineering liquid-vapor phase transition using nanoporous graphene (water for all). Prof. Ganapathy Ayyappa. CODEV Seed money. Grant EPFL Lausanne. Ongoing.